NAVY DEPARTMENT
THE DAVID W. TAYLOR MODEL BASIN
WASHINGTON 7, D.C.

[redacted]

TESTS OF THE ELASTIC STABILITY OF A RING-STIFFENED CYLINDRICAL SHELL, MODEL BR-5 (λ = 1.705), SUBJECTED TO HYDROSTATIC PRESSURE

by

Robert C. Slankard and
William A. Nash, Ph. D.

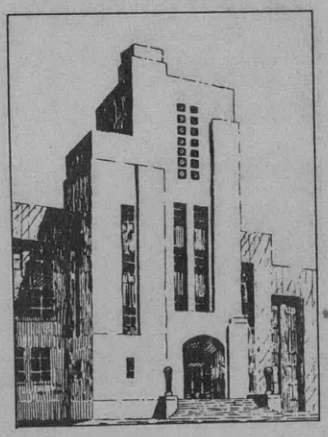

May 1953

Report 822

NS 731-038

TESTS OF THE ELASTIC STABILITY OF A RING-STIFFENED CYLINDRICAL SHELL, MODEL BR-5 (λ = 1.705), SUBJECTED TO HYDROSTATIC PRESSURE

by

Robert C. Slankard and William A. Nash, Ph.D.

May 1953

Report 822
NS 731-038

TABLE OF CONTENTS

ABSTRACT

Model BR-5 was the second in a series of experimental models to be used in the investigation of the elastic stability of the shell component of ring-reinforced cylinders subject to external hydrostatic pressure. This model was intended to be a duplicate of the first model, BR-1, to check on repeatability of test results. The pressures at which the first lobe formed in each of the two models were identical, although the maximum load-carrying capacity of BR-5 was slightly less than that of BR-1.

An automatic recording deflectometer was used during the test to record circularity. From a study of the circularity plots at each station, the following observations may be made:

(a) at each ring the inward radial displacement was fairly uniform around the periphery of the model, and

(b) for those stations located midway between rings in the four equal bays of the model, the radial displacements were, for the most part, exaggerations of the initial no-load contours.

An examination of the lobe formation during the test and an inspection of the pictures indicated that the lobes in adjacent bays were staggered. Furthermore, with such stagger, there was virtually no rotation of the generator at the two frames bounding a lobe. This mode of deformation differs considerably from the von Mises assumption of no rotational restraint at the edge of a finite cylinder but is in agreement with one of the analyses of Salerno and Levine.

The von Mises' theory for predicting the buckling pressure of a cylindrical shell of finite length having the geometry of BR-5 and subject to hydrostatic pressure yields a minimum value of 123 psi for a buckled configuration of 16 lobes. The experimentally determined buckling pressure for Model BR-5 was 80 psi with a buckled configuration of 14 lobes. Permanent set after removal of the pressure of 80 psi was evident in the regions of the first three lobes in Model BR-5. Initial out-of-roundness and residual welding stresses are possible explanations of the deviation of the experimental from the theoretical result.

INTRODUCTION

An experimental investigation of the elastic stability of the shell component of ring-reinforced cylinders has been initiated at the David Taylor Model Basin to develop a more comprehensive understanding of this phenomenon. The instrumentation and procedures adopted for these tests of approximately 12 ring-reinforced cylinders are intended to develop necessary information concerning both buckling pressures and buckling configurations on the basis of which a rigorous theory could be validated.

The second model tested, BR-5, had a "thinness ratio" λ of 1.705* (Reference 1).[1] It was very nearly a duplicate of the first model, BR-1 (Reference 2, page 37), however, the technique used in welding the rings to the shell was modified on BR-5 because of the undesirable initial out-of-roundness of BR-1. Hence the second model did not serve as a control on shop methods in all respects.

In this report Model BR-5 is described, the progressive failure of the model under increasing hydrostatic pressure is demonstrated by photographs and circularity contours, and the results of this test are discussed and compared with the results of tests of Model BR-1. A brief discussion of the automatic recording deflectometer used to obtain the circularity contours of Model BR-5 is given in Appendix 1.

DESCRIPTION OF MODEL

Model BR-5 was a ring-stiffened cylindrical shell with four equal bays; the geometric characteristics** were:

$2R = 26.750$ in.	$L_f = 5.27$ in.
$h = 0.062$ in.	$L = 4.92$ in

Here 2R is the diameter to the median surface of the shell, h is the thickness of the sheet before rolling, L_f is the center-to-center distance between adjacent rings, and L is the distance L_f diminished by (a) the thickness of one ring and (b) two-thirds the axial dimension of both of the welds joining the rings to the shell. With the above dimensions and a yield strength of 54,400 psi, the thinness ratio λ, is 1.705.

A schematic diagram of Model BR-5 is shown in Figure 1. During fabrication a bulkhead ring was used at one end to hold the model to circular shape. The model was closed at

---

[1] References are listed on page 37.

* $\lambda = \sqrt[4]{\frac{\left(\frac{L}{2R}\right)^2}{\left(\frac{h}{2R}\right)^3}} \sqrt{\frac{\sigma_y}{E}}$

where L is the unsupported length of cylindrical shell,
R is the mean radius,
h is the shell thickness,
E is the modulus of elasticity, and
σ_y is the yield point (compressive).

** The parameters describing Model BR-1 were 2R = 26.753 in., h = 0.065 in., L = 4.92 in., λ = 1.82 and σ_y = 61,700 psi.

one end by a heavy stiffened closure plate and was welded at the open end to a heavy serrated ring used for mounting the model in the hydrostatic test chamber.

The cylindrical shell of the model was fabricated on a mandrel having an outside diameter of 26.688 in. The shell was rolled from a 1/16-in. (nominal thickness) sheet of Alan Wood steel, and the rings were made from high tensile steel plating. The 1/16-in. steel sheet used for the shell plating was sand-blasted with ordinary silica and then cold-rolled to within approximately 0.01 in. of the radius of the mandrel. Shell thicknesses were measured before rolling; the average shell thickness was 0.062 in. The shell plating was held in position on the mandrel by three clamping bands drawn tight by bolts while the longitudinal seam of the model was being welded. This weld closed the gap of approximately 1/32 in. which existed in the shell after the bands had been drawn tight. After the weld had been dressed down to be flush with the shell plating, the rings were placed on the model and welded in a sequence intended to produce minimum distortion of both shell plating and rings. This initial distortion arising in the construction of Model BR-1 was so marked that it was decided to change both the welding sequence and the order in which the rings were placed on the model during construction of BR-5. The procedure followed in welding the rings to the shell is shown in Figure 2.

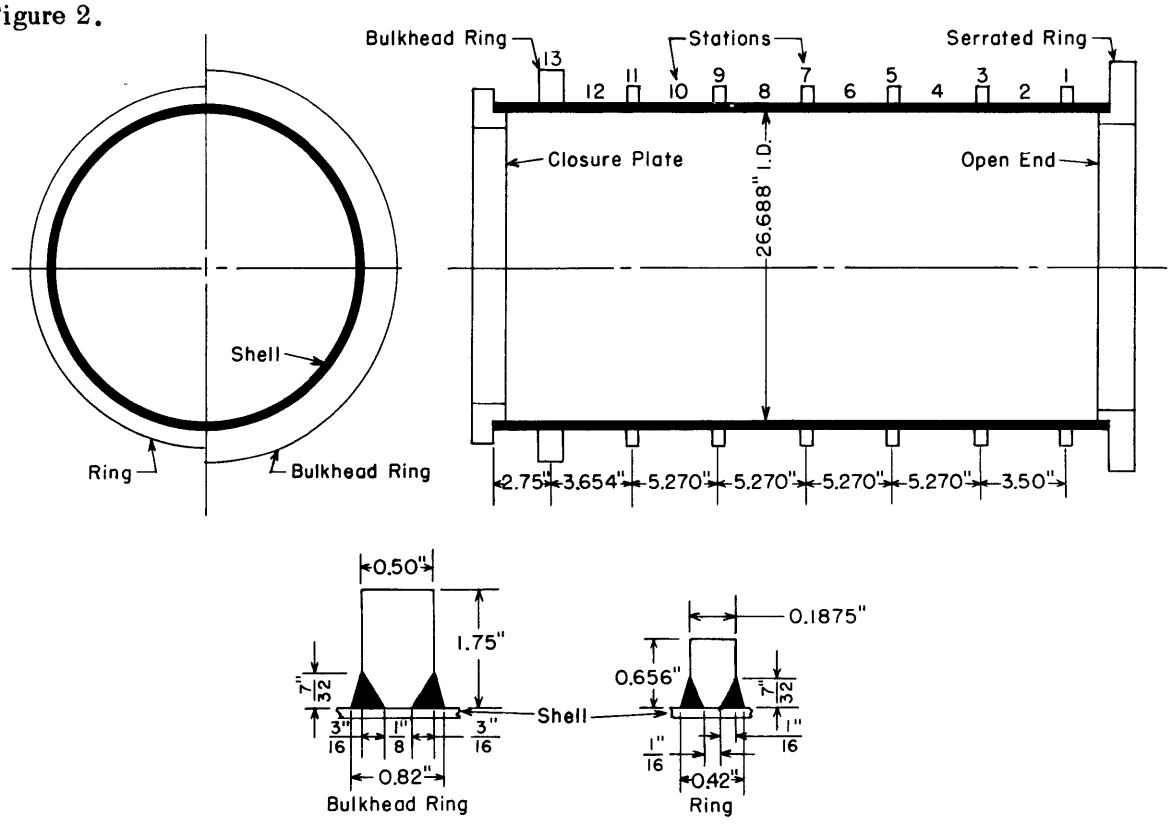

Figure 1 - Schematic Drawing of Model BR-5

It is to be noted that the corners of the rings in contact with the shell plating were undercut, as shown in Figure 1, so that the faying width of the rings would exceed the desired thickness of the rings (3/16 in.) by a minimum amount. Upon completion of the model, it was

found that the average faying width of the rings was 0.42 in. and that of the bulkhead ring 0.82 in. This distance was measured from toe to toe of the welds.

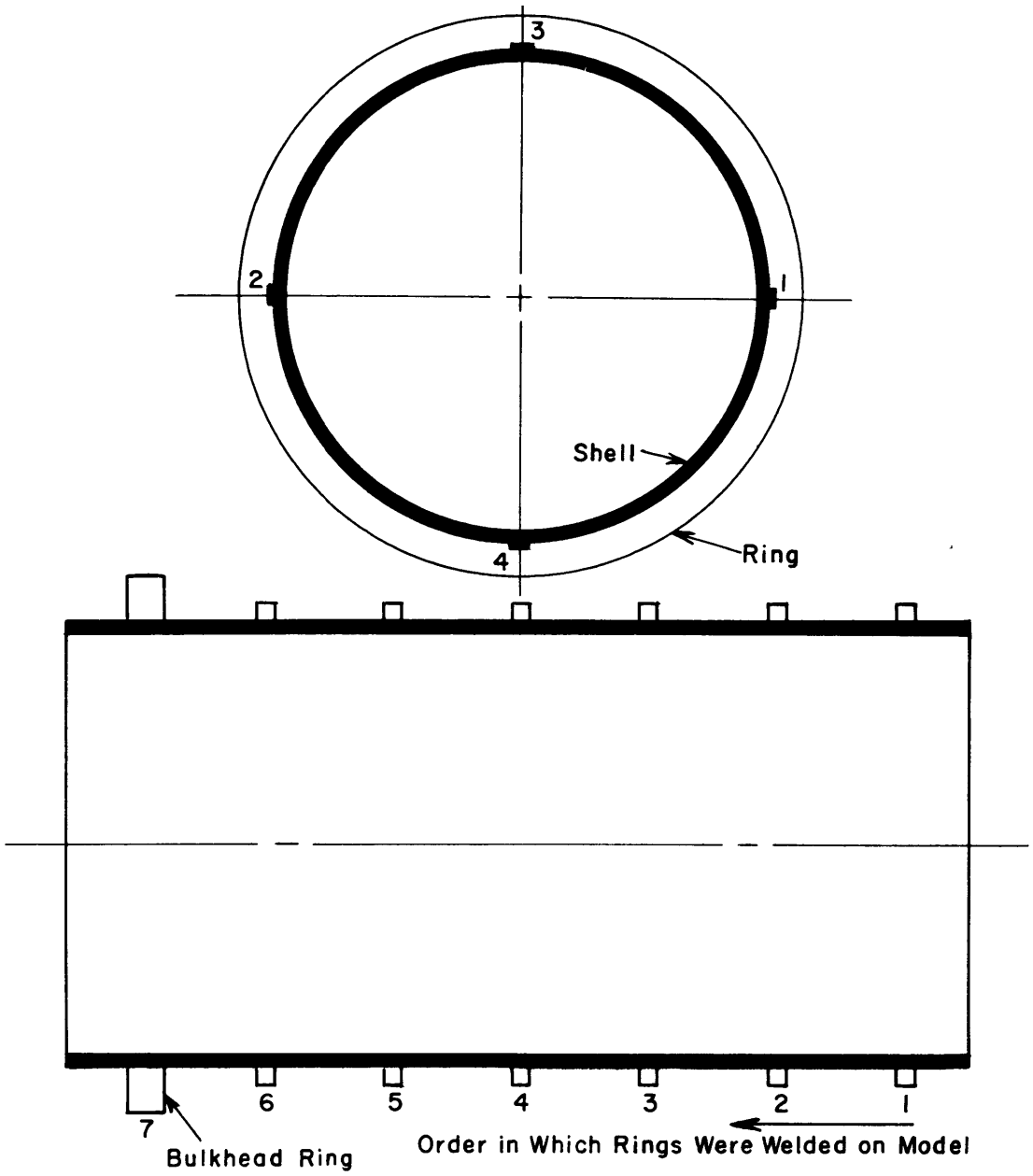

Figure 2 - Welding Sequence for Model BR-5

A four-point welding sequence was used in placing the rings on Model BR-5 instead of the eight-point welding sequence used in constructing Model BR-1 (Reference 2) to reduce the initial distortion that was found to be present in BR-1. In the four-point welding sequence the weld was started over a length of about 3 in. on both sides of the ring (Point 1) and then continued for a length of 3 in. at a point 180 deg from Point 1, i.e., Point 2. Next welding was started at Point 3, which is 90 deg from Point 1, and then at Point 4, which is 180 deg from Point 3; the length of both welds was equal to that of the first weld. Welding was then continued in a counterclockwise direction in each of the four unwelded regions until the ring was secured to the shell. The rings were placed on the model by first welding Ring 1 to the shell and then moving along the length of the model toward the bulkhead ring with Rings 2, 3, 4, 5. and 6, respectively.

To check the yield strength, ten specimens of the shell plating, 2 3/8 in. long and 1/2 in. by 1/16 in. in cross section, were cut from the flat sheet before it was rolled into a cylinder. Six of these specimens were cut with the long dimension in the direction of rolling (longitudinal specimens), and the remaining four specimens were cut with the long dimension in the direction perpendicular to rolling (transverse specimens). The average compressive yield point in the direction of rolling of the sheet was 52,600 psi; that in a transverse direction was 57,100 psi. The mean compressive yield point without regard to direction of rolling was thus 54,400 psi. Since no accurate determination of the compressive modulus of elasticity was made with these specimens, the value of 30.5×10^6 psi determined previously for similar sheet[3] was accepted as a nominal value.

It was stipulated in the Taylor Model Basin specifications[4] for construction of the model, that the out-of-roundness of the ring-reinforced shell was not to exceed one-half the shell thickness. The out-of-roundness was defined as the difference between the maximum and minimum distances of the shell from a circle centered so that it best fitted the contour of the shell.

By the criterion for the measurement of out-of-roundness proposed by Holt[5], Model BR-5 displayed an out-of-roundness of 0.0232 in. Thus the maximum ratio of eccentricity to shell thickness according to Holt's criterion, is 0.374; this occurred at Station 4. Holt's criterion indicates that the initial circularity of Model BR-5 was better than that of Model BR-1, which had a maximum ratio of eccentricity to shell thickness of 1.023.

TEST APPARATUS

Circularity for Model BR-5 was measured by means of an automatic recording deflectometer (see Appendix 1). This deflectometer, which replaced a manually operated deflectometer, was specially designed and built to conserve time required to take circularity data and to provide a means of recording circularity data from outside the new 8-ft pressure tank at the Taylor Model Basin.

Model BR-5 was tested in the 37-in. diameter, 1500-psi pressure tank at the Taylor Model Basin. Oil was used as a pressure medium, and pressure was applied to the external surface of the shell by means of a manually operated pump. In order to expedite testing, displacement data were taken only at the upper six stations at any one pressure increment and only at the remaining seven stations at the succeeding pressure increment; the sequence is indicated in Table 1. Several runs were made to minimize nonlinearity in the final application of load leading to failure.

The hydrostatic pressure exerted upon the exterior of the shell was measured by means of an elastic-tube pressure gage calibrated so that a reading of 1 μ in./in. of strain corresponded to a pressure of 1 psi on the model. Since the strains indicated by the elastic-tube pressure gage were read on an SR-4 strain indicator, the pressure could be measured only to the nearest 5 psi. The hydrostatic pressure was also measured during the test by means of a

Bourdon gage which had been calibrated on a dead-weight tester before the model test was started. The smallest subdivision on the dial of the Bourdon gage corresponded to a pressure increment of 5 psi. With this sensitivity, pressure increments of 2.5 psi could be determined. Although this accuracy is adequate for these tests, even greater precision would have been desirable. All pressures reported during the test were read from the elastic-tube gage and checked by the Bourdon gage.

TABLE 1

Pressure Increments of Test of Model BR-5

Run 1		Run 2		Run 3		Run 4	
Pressure psi	Stations at which deflections were taken	Pressure psi	Stations at which deflections were taken	Pressure psi	Stations at which deflections were taken	Pressure psi	Stations at which deflections were taken
0	1 - 13	0		0		0	
20	7 - 13	20		20		80	4,6,8,10
40	1 - 6	40		40		85	
		50	7 - 13	50		90	
		60	1 - 6	60		95	
		70	7 - 13	70			
				80	1 - 13	Failure	
				0	3,4,5,6,10		

TEST PROCEDURE AND RESULTS

Before external pressure was applied to the model, circularity contours were obtained by means of the recording deflectometer so that the initial out-of-roundness would be known at stations located under the rings (odd-numbered stations in Figure 1) and midway between the rings (even-numbered stations in Figure 1). A typical circularity contour for a station midway between the rings is shown in Figure 3. A complete set of contours are shown in Figures 20 through 32 in Appendix 2. As can be seen from these figures, the initial out-of-roundness of the model was more pronounced at the stations midway between the rings than at the stations under the rings and definite regions existed in the model of maximum inward radial distortion and of maximum outward radial distortion. At any one station these regions were separated by approximately the same central angle, but they did not occur at the same angular orientation in the various bays. It is interesting to note, too, that in this model the initial contours were indicative of the number of lobes formed in the model under pressure.

The area under the no-load contour at each station was determined with the aid of a planimeter, and the radius of a circle with this same area was calculated. With the introduction of a scale factor (determined by the magnification used) the radius of the circle obtained by planimetering may be converted to the mean inside radius of the model at the corresponding

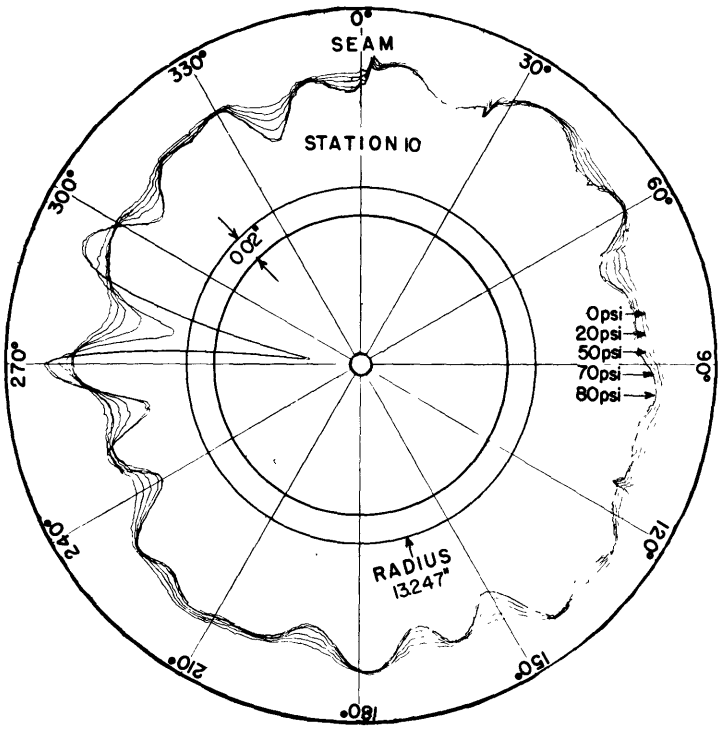

Figure 3 - Progressive Contours of the Shell of the Model Midway Between Stations 9 and 11

Note that those regions which were initially distorted inwardly continued to deform inwardly under increasing pressure.

station. This latter radius is denoted by R_a in Table 2. Circularity contours obtained at the various stations during the test of Model BR-5 are shown in Figures 20 through 32 in Appendix 2. The regions of initial inward and outward radial distortion of shell plating did not, in general, extend from one bay into the adjacent one. There were 12 regions initially distorted inward at Station 4, 12 at Station 6, 10 at Station 8, and 10 at Station 10. By Holt's method for measurement of out-of-roundness,[5] the maximum out-of-roundness for Model BR-5 was 0.0232 in. located 119 deg from the seam at Station 4. The maximum inward and outward measurements of out-of-roundness for each station as indicated by Holt's method are given in Table 3.

In order to evaluate the circularity contour charts, two concentric circles were drawn on each chart to furnish a base for absolute as well as relative measurements. The larger circle represents a radius of 13.247 in., and the smaller circle represents a radius of 13.227 in. The difference between these two radii, 0.02 in. measured on the model, corresponds to 1.0 in. on the charts for which the recording magnification was 50. The two circles were drawn on each of the circularity charts to provide an absolute scale and to furnish sufficient data for determining the actual radius of the model at any point.

During the first three pressure runs described in Table 1, the pressure was increased at the rate of 10 psi over a 1-min interval and was then held constant for one additional minute before pressure was again increased. A 5-min interval elapsed between the end of Run 1 and the beginning of Run 2, and also between the end of Run 2 and the beginning of Run 3. In Run 3 the pressure was increased by increments of 10 psi/min until 80 psi was reached, at which time three lobes appeared in the cylindrical shell. These lobes were at 119 deg

TABLE 2

Mean Interior Radius at Each Station for Model BR-5

Station	R_a in.
2	13.3209
3	13.3122
4	13.3233
5	13.3136
6	13.3249
7	13.3150
8	13.3269
9	13.3211
10	13.3317
11	13.3195
12	13.3285

TABLE 3

Points of Maximum Out-of-Roundness for Model BR-5 by Holt's Method

Station	Out-of-Roundness in.	Direction	Location from Seam deg
4	0.0198	Outward	190
	0.0232	Inward*	119
6	0.0158	Outward	170
	0.0182	Inward*	320
8	0.0172	Outward	300
	0.0182	Inward	80, 220
10	0.0148	Outward	180
	0.0212	Inward*	280

*These are the points of maximum out-of-roundness in the model; it was at these points that the three lobes formed at 80 psi.

from the seam at Station 4, 320 deg from the seam at Station 6, and 280 deg from the seam at Station 10. Thus 80 psi was the buckling pressure for Model BR-5. After the circularity contours had been obtained at all stations at a pressure of 80 psi, the pressure was reduced to zero, and the circularity was taken in the regions of these three lobes at Stations 3, 4, 5, 6, and 10 to determine the residual radial deformation (see Table 4). In Run 4 the pressure was increased at a rate of 10 psi/min to a value of 80 psi, at which pressure the same three lobes appeared as before. Circularity was then measured at Stations 4, 6, 8, and 10.

Upon completion of these measurements, the deflectometer was used to obtain circularity contours at various positions along the lobe which occurred at 119 deg from the seam between Stations 3 and 5. These contours, which were recorded using a magnification factor of 25, are shown in Figure 4. The contours shown in Figure 4a represent the entire lobe between Stations 3 and 5. The "off-set" contours shown in Figure 4b represent that half of the lobe between Stations 4 and 5; they have been plotted in the same manner as those shown in Figure 4a except that the origins of each of the plots have been translated along a radial line so that the contours do not overlap. The symmetry of this lobe is evident from a study of Figures 4a and 5.

TABLE 4

Maximum Radial Displacements at 80 psi - Run 3

Station	Maximum Radial Displacement (Δ) in.	$\frac{\Delta}{h}$ in.	Orientation (deg from seam)	Permanent Set at End of Run 3 in.
1	0.006	0.0968	90	
2	0.014	0.2258	110	
3	0.008	0.1290	120	
4	0.154	2.4839	119	0.096
5	0.010	0.1613	119	0.007
6	0.056	0.9032	315	0.032
7	0.007	0.1129	100	
8	0.029	0.4677	340	
9	0.008	0.1290	75	
10	0.148	2.3871	280	0.099
11	0.005	0.0806	90	
12	0.015	0.2419	185	
13				

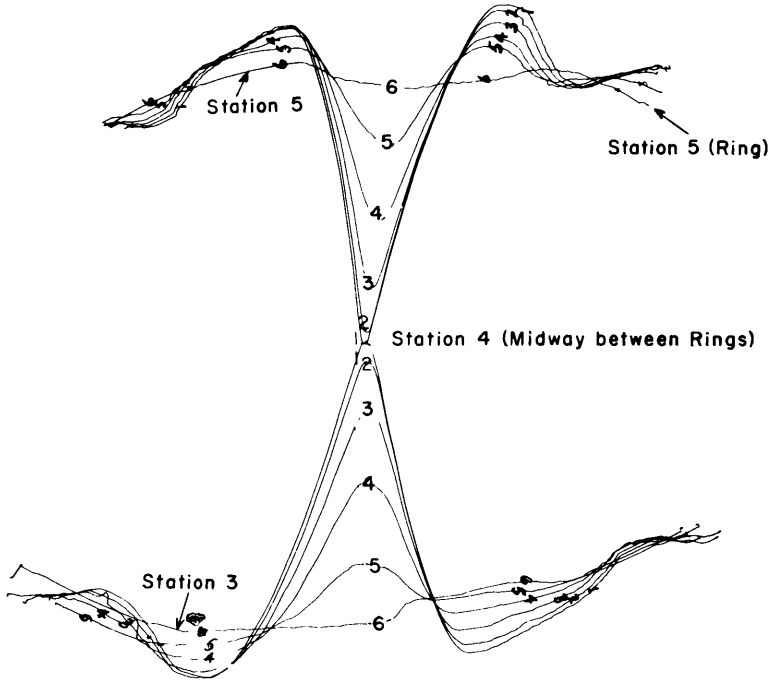

Figure 4a - Contours Between Stations 3 and 5

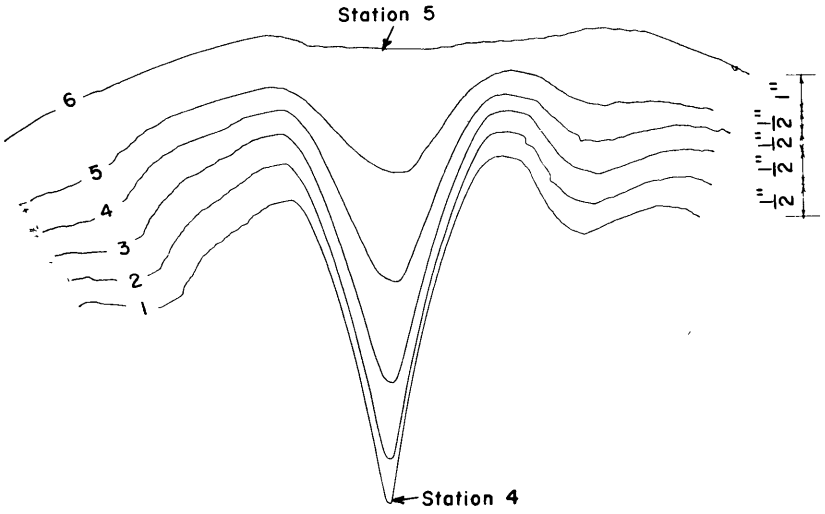

Figure 4b - Contours Between Stations 4 and 5
Displaced to Eliminate Overlap

Figure 4 - Lobe Contours 119 deg from Seam at Pressure of 80 psi

The distances between the various contours are as follows:

(a) Contour 1 was the peak of the lobe which occurred at Station 4,

(b) Contour 2 was 7/ 16 in. from Contour 1, (measured along a generator of the shell),

(c) Contour 3 was 1/2 in. from Contour 2,

(d) Contour 4 was 1/2 in. from Contour 3,

(e) Contour 5 was 1/2 in. from Contour 4, and

(f) Contour 6, which corresponds to the station at the ring, was 3/4 in. from Contour 5.

The recording probe was then removed, and the pressure was raised from 80 psi to 85 psi with the appearance of 4 additional lobes; from 85 psi to 90 psi six additional lobes appeared, and from 90 psi to 95 psi 23 additional lobes. The pressure of 95 psi was the maximum load-carrying capacity of the model. Although pumping of the oil was continued after this pressure had been reached, the pressure immediately decreased to a value of 90 psi and

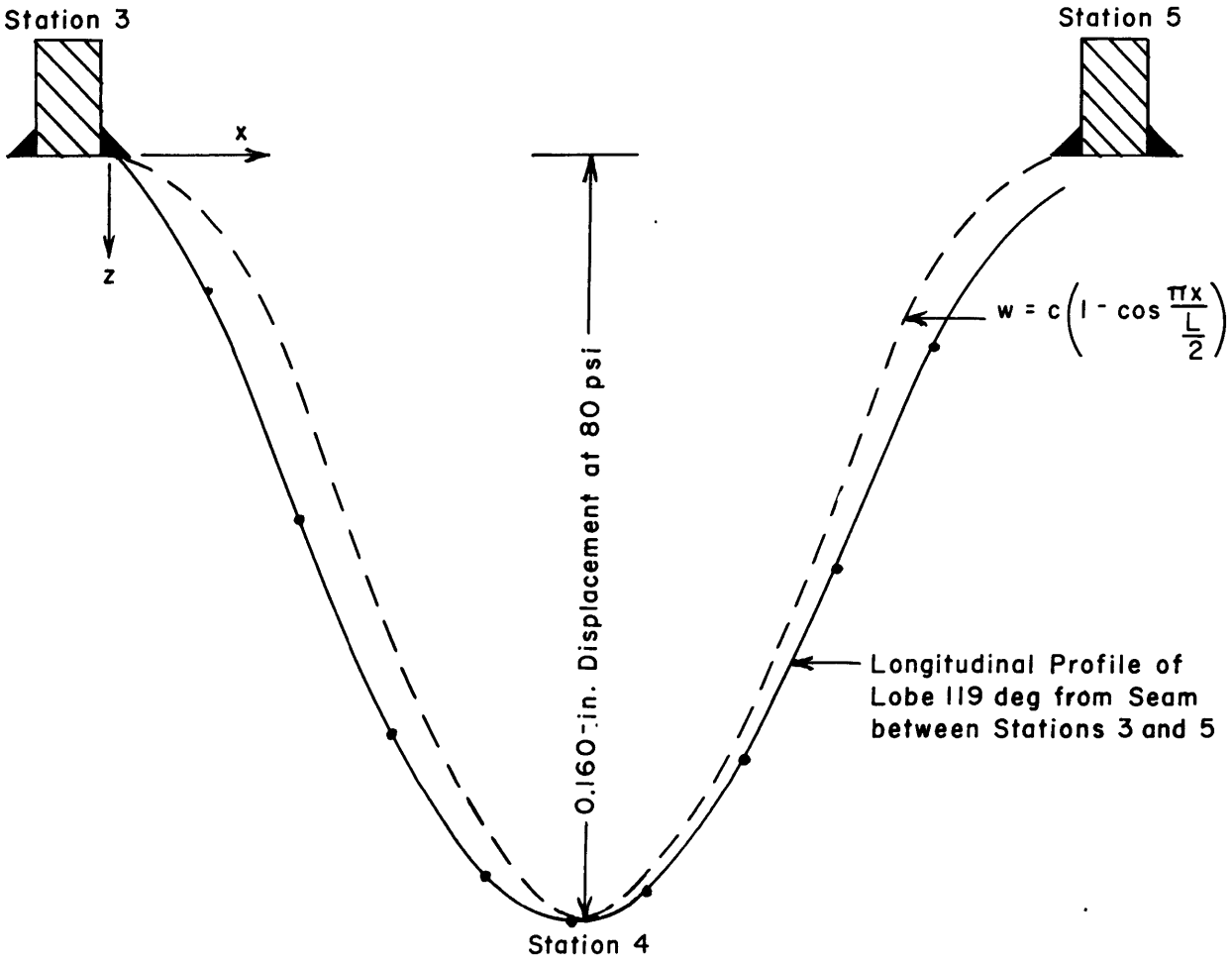

Figure 5 - Comparison of Longitudinal Profile of Lobe 119 Degrees from Seam Between Stations 3 and 5 with Theoretical Curve

remained constant for several minutes before decreasing again. Thirty minutes after the pressure of 95 psi had been attained, the pressure was 55 psi even though pumping had been continued throughout this time interval.

During this time the amplitude of each of the lobes increased with continued pumping, as did the number of lobes in several of the bays. The maximum number of lobes in any of the four equal bays was 13, although it was evident that there was space for 14 lobes in that bay. This number of lobes corresponds to a central angle of 26 deg for each lobe. The number of lobes in the various bays at several pressures during the test, as well as the number remaining after the removal of pressure at the conclusion of testing, is tabulated in Table 5. When the pressure had dropped to 55 psi pumping was discontinued, the pressure was released, and the test was terminated because of excessively large deformations of the model. The variation of the ratio of radial displacement to shell thickness with pressure is shown in Figure 6 for 14 points located around the periphery of Station 10. These graphs suggest that those regions initially distorted inward were displaced further inward with a smooth displacement curve and those regions initially distorted outward tended to deflect further outward with an irregular displacement curve.

TABLE 5

Number of Lobes in Various Bays at Several Pressures

Run 4 Pressure psi	Number of Lobes Between Stations					
	Stations 1 and 3	Stations 3 and 5	Stations 5 and 7	Stations 7 and 9	Stations 9 and 11	Stations 11 and 13
80	0	1	1	0	1	0
85	0	1	1	3	2	0
90	0	2	3	4	4	0
95*	0	10	7	10	9	0
90	0	11	12	11	9	0
85	0	12	12	11	11	0
70	(No new lobes)					
60	(No new lobes)					
0 (end of test)	0	12	13	12	12	0

*Highest pressure that was reached during the test. Additional pumping increased the number of lobes and their size but was accompanied by a decrease in pressure.

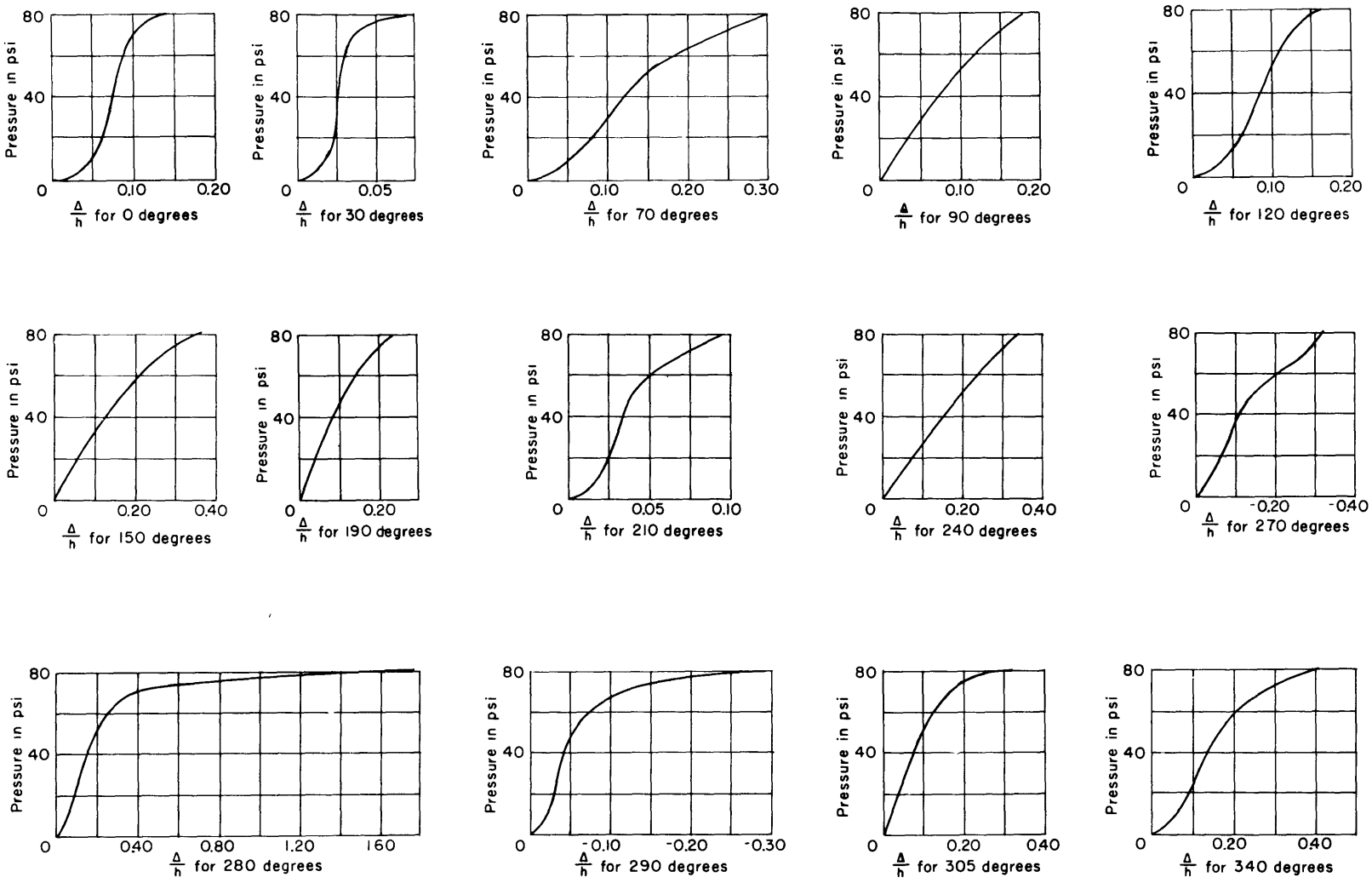

Figure 6 - Pressure Plotted Against Ratio of Radial Displacement to Shell Thickness at Station 10

DISCUSSION OF RESULTS

From a study of Figures 20 through 32 (Appendix 2) and from a consideration of the values of out-of-roundness given in Table 3, it is apparent that the greatest initial eccentricity existed at Station 4. Stations 4 and 6 had the maximum number of initial inward distortions. The mean inward radial displacement per unit pressure at Stations 2 through 12 is tabulated in Table 6 and shown graphically in Figure 7. These results were obtained from data taken at pressures not exceeding 70 psi since that was the highest pressure at which linear action of the model was observed. In fact, the mean inward displacement was first computed using the pressure interval from 0 psi to either 40 or 50 psi (depending upon the particular station) and then using the interval from 0 psi to either 60 or 70 psi. The displacements per unit pressure were different in these two cases, as shown in Figure 7. The mean of these two computed values at each station is shown in Table 6. There seems to be little explanation of this irrational behavior. One possible reason could be the effect of residual welding stresses in the model; another could be some undetected fault in the recording deflectometer. A somewhat similar behavior was noticed during test of Model BR-1. From Table 6, the mean inward radial displacement at the rings bordering the four equal bays was 0.000025 in. per unit pressure, while at the stations midway between these rings it was 0.000086 in. per unit pressure. At the bulkhead ring and also at Station 1, the radial displacements shown on the circularity charts were too small to measure with accuracy.

Permanent set after removal of the pressure of 80 psi (at the end of Run 3) is evident in the regions of the first three lobes as may be seen from Figures 23, 25, and 29. From this

TABLE 6

Mean Inward Radial Displacements at Various Stations*

Station	Displacement per psi in.
2	0.00006322
3	0.00002501
4	0.00007469
5	0.00003277
6	0.00008250
7	0.00003350
8	0.00009595
9	0.00001287
10	0.00010000
11	0.00002041
12	0.00010174

*Displacements given are those obtained from pressures of 40 - 50 and 60 - 70 psi.

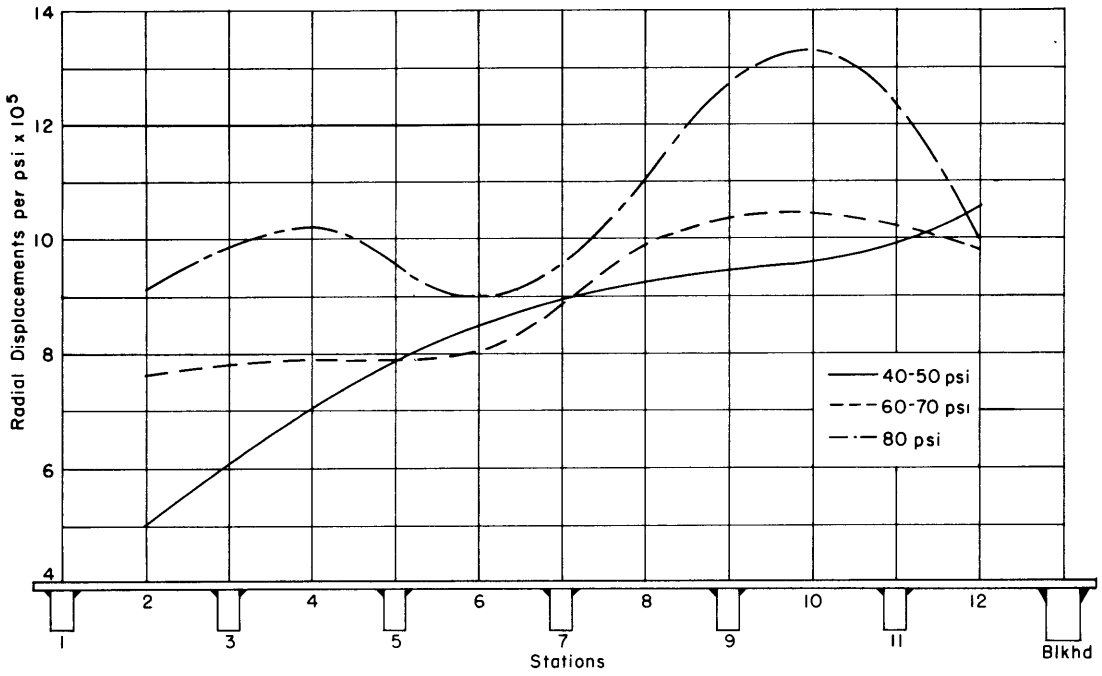

Figure 7a - Stations Midway Between Rings

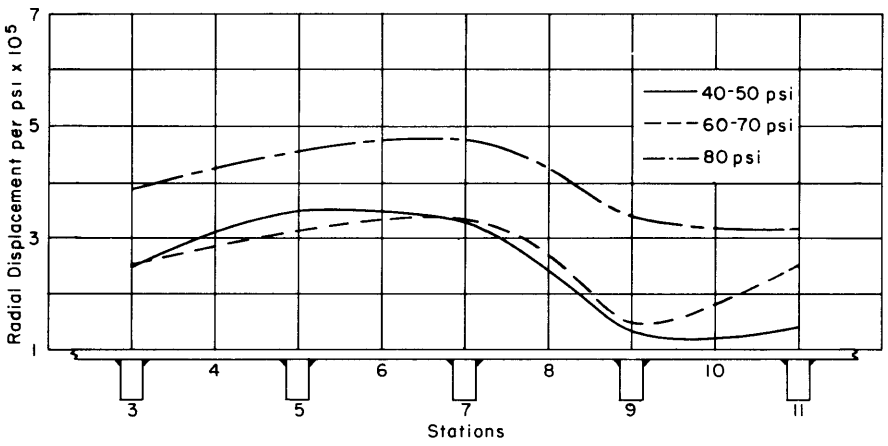

Figure 7b - Stations Directly Under Rings

Figure 7 - Curves of the Average Radial Displacements at Longitudinal Stations

it may be concluded that none of these lobes was confined to the elastic range of action of the material. All three of these lobes were formed by the continued increase in amplitude of the initial inward distortions existing at those regions with no-load acting on the shell. Table 4 gives the maximum radial displacement at each station for a pressure of 80 psi and also the permanent set (after removal of pressure) at the corresponding points for Stations 4, 5, 6, and 10.

The longitudinal profile along the central line of the lobe at 119 deg from the seam between Stations 3 and 5 may be determined from Figure 4a. This experimentally determined profile is plotted as a solid line in Figure 5. On this same figure there is also plotted the function

$$w = C\left(1 - \cos\frac{\pi x}{\frac{L}{2}}\right)$$

where w is the radial component of displacement of a particle in the median surface of the shell and x is the longitudinal coordinate measured from the third point of the weld as shown in Figure 5. (In this report it has been assumed that the third of the weld toward the center of the bay offers no support to the shell.) For Model BR-5, L equals 4.92 in. It is apparent that this function is a fairly good approximation to the buckled configuration.

The following observations may be made from a further study of Figures 20 through 32:

1. At each ring the inward radial displacement was fairly uniform around the periphery of the model, the maximum occurring 150 deg from the seam.

2. For those stations located midway between rings in the four equal bays of the model, the initial no-load contours of the model were, for the most part, qualitatively preserved as the pressure increased. The regions that were originally distorted inwardly moved toward the center of the model, while those initially distorted outwardly tended to remain at those same initial points without any noticeable outward displacement. However, at points on either side of each of the three lobes recorded at 80 psi, there were outward radial displacements at regions which had initially been distorted inwardly.

After the pressure had increased to a value sufficient to cause the formation of lobes, it was noticed that the closure plate at the end of the model had become skewed with respect to the longitudinal axis. As the pressure was increased, the longitudinal distances that once identified the 13 stations were no longer valid.

The history of the lobe formations leading to failure of the shell may be seen in Figures 8 and 9. In Figure 8c, 20 lobes are visible, 5 in each of the four equal bays. It is interesting to note how evenly the lobes have formed in the shell, yet in adjacent bays the lobes are staggered in such a manner that they have the same circumferential spacing and angular orientation around the periphery in alternate bays. This same phenomenon was observed for Model BR-1. Without a further increase in pressure, the lobes continued to increase both in

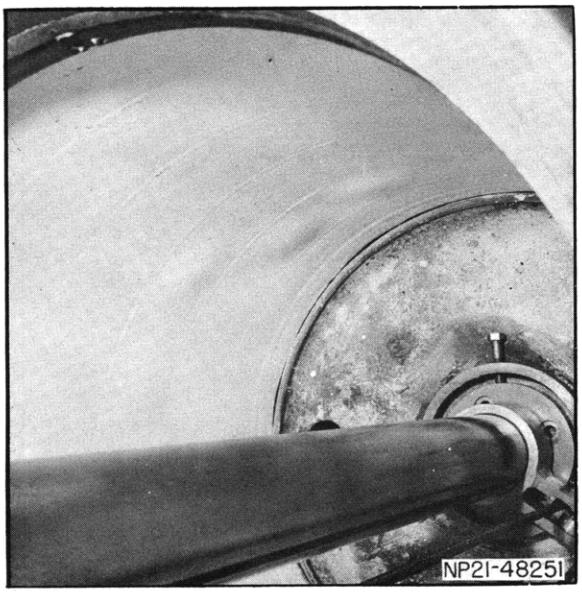

Figure 8a - At 85 psi

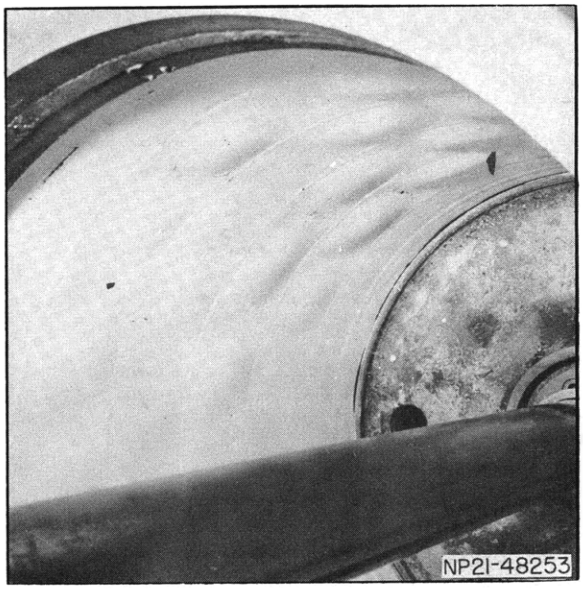

Figure 8b - At 90 psi

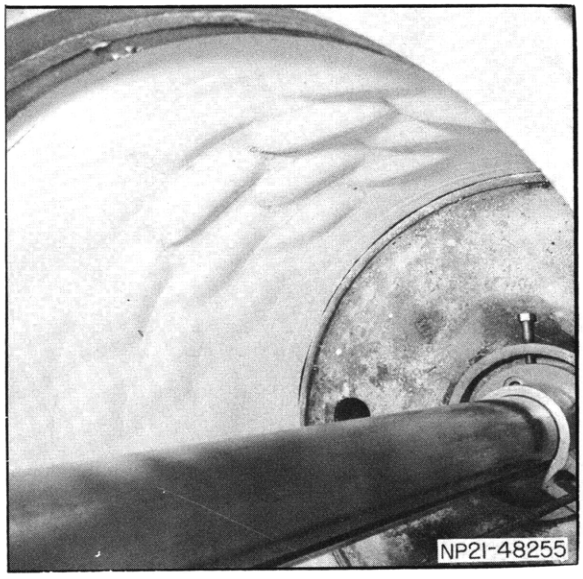

Figure 8c - At 95 psi

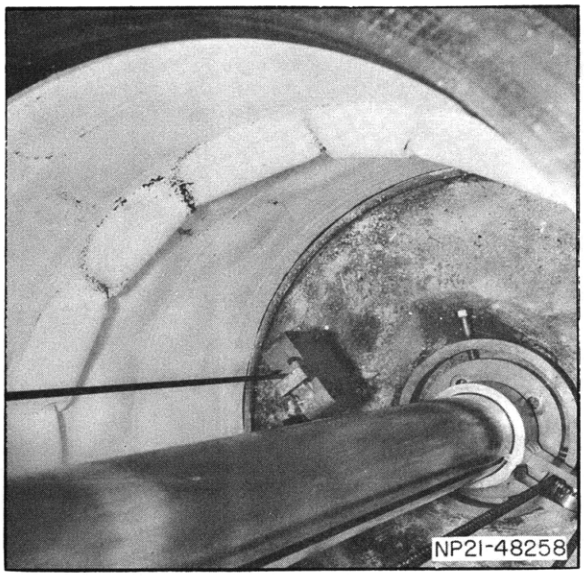

Figure 8d - At 55 psi

Figure 8 - Progressive Formation of Lobes as Pressure Increased in Final Run

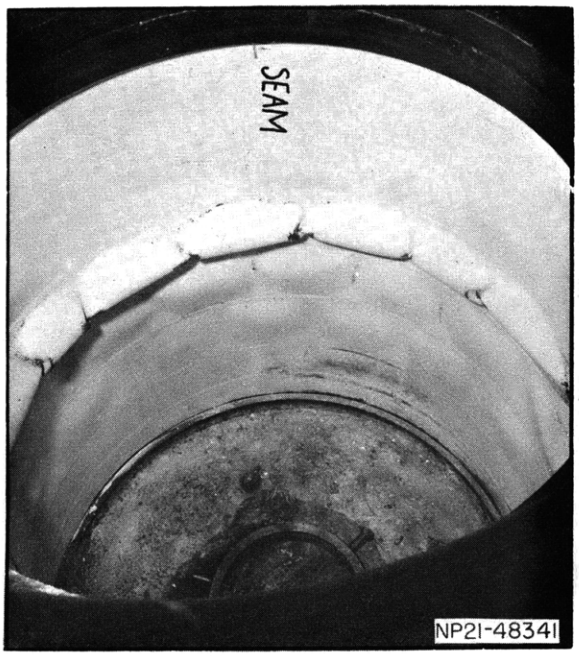

Figure 9a - At Seam

Figure 9b - At 90 deg

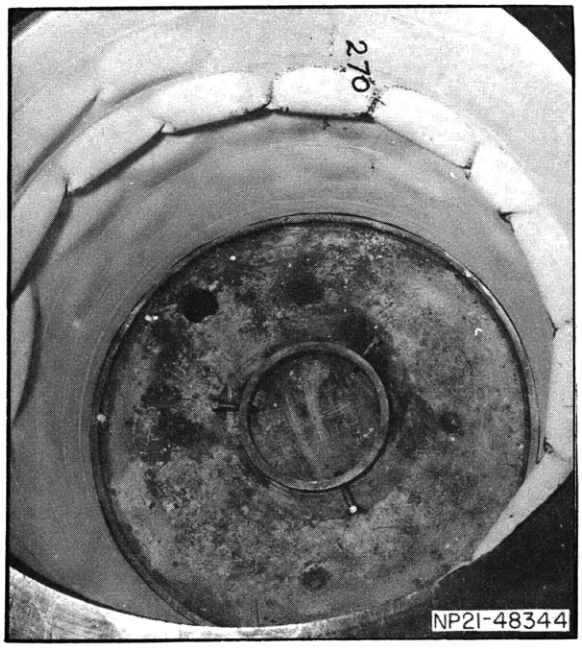

Figure 9c - At 270 deg

Figure 9 - Photographs of Lobes After Release of Pressure and Removal of Deflectometer

number and amplitude until their amplitudes finally became excessive in the bay between Stations 5 and 7. This is shown in Figures 8 and 9. This failure was characterized by a chain of 13 interlocking lobes with additional dormant lobes in the surrounding bays. There was just enough room left in this bay for another lobe which would have given a total of 14. Nine of the 13 lobes that were actually formed in the bay between Stations 5 and 7 may be seen in Figure 9c.

COMPARISON OF RESULTS WITH THEORY

BUCKLING PRESSURE

Figure 10 shows the variation in number of lobes with pressure as determined by the von Mises' equation. The von Mises'[6] theory for predicting the buckling pressure of a cylindrical shell of finite length having the geometry of Model BR-5 and subject to hydrostatic pressure yields a minimum buckling pressure of 123 psi for a buckled configuration of 16 lobes. The Experimental Model Basin formula[1], a simplification of von Mises' work, yields a buckling pressure of 129 psi, and Tokugawa's theory[7] predicts a buckling pressure of 134 psi with either 15 or 16 lobes. In each of these theories, only the elasticity of the shell plating is considered, and the effect of the reinforcing rings upon the elastic behavior and stability strength is completely disregarded; hence it is uncertain that these theories should apply with any degree of accuracy to a ring-reinforced cylindrical shell. Model BR-5 buckled at a pressure of 80 psi with a configuration of 14 lobes.

The von Mises' theory for predicting the buckling pressure yields a value of 134 psi for a buckled configuration of 14 lobes. This is the number of lobes that would have formed in the model if the buckling deformations had been axisymmetric. In reality the greatest number of lobes that formed in any one of the four equal bays was 13.

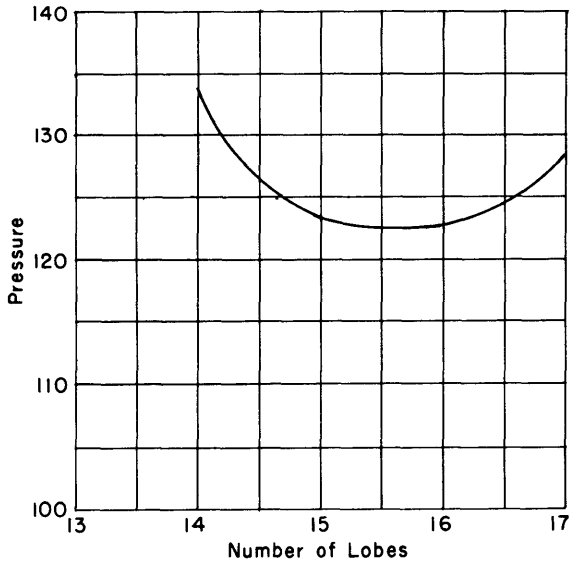

Figure 10 - Variation in Number of Lobes with Pressure as Computed by von Mises' Equation

The effect of the rings on stability strength of cylindrical shells has been considered in theories developed by Salerno and Levine.[8] In one of a series of papers, Salerno assumed a displacement pattern at buckling corresponding to rigid end supports of the shell. The reinforcing rings were taken to be infinitely rigid; hence no strain energy was absorbed by them. This analysis, applied to Model BR-5, yields a buckling pressure of 173 psi with a buckled

configuration involving 15 or 16 lobes. This value was regarded by Salerno as constituting an upper limit to the hydrostatic buckling pressure of an infinitely long, circular, cylindrical shell reinforced by evenly spaced rings. In another paper of this series, Salerno presented a theory that predicts a buckling pressure of 168 psi for a model having the geometry of BR-5. This theory assumes that the only displacement of the rings consists of bending out of their own planes.

OUT-OF-ROUNDNESS

The values of buckling pressure obtained by the various theories pertain to a geometrically perfect, circular, cylindrical shell. Since the model tested exhibited a marked out-of-roundness before the pressure was applied, it was necessary to apply a correction factor to each of these theoretical pressures. The maximum initial out-of-roundness occurred 119 deg from the longitudinal seam at Station 4 with an initial deviation from true circularity of 0.0232 in. Thus the maximum ratio of eccentricity to shell thickness was 0.374. A semi-rigorous analysis of the reduction in buckling pressure because of initial deviation from true cularity in an initially out-of-roundness cylinder. Sturm's analysis for the reduction in buckling pressure due to initial out-of-roundness presupposes the method for measurement of out-of-roundness advanced by Holt.[5] As applied to Model BR-5, the reduction in buckling pressure for various values of the ratio of eccentricity to shell thickness is plotted in Figure 11. From this plot it may be seen that an eccentricity-thickness ratio of 0.374 corresponds to buckling pressures of 77 psi for 16 lobes (lower curve), 92 psi for 14 lobes (middle curve), based upon von Mises' values, and 107 psi (upper curve) based upon Salerno's theory. As noted in the previous section, the first lobe formed at 80 psi. The 92-psi theoretical buckling pressure, for 14 lobes, was 15 percent higher than the experimental pressure of 80 psi. It should be noted, however, that the von Mises' equation neglects the effect of the rings on the stability strength of the cylindrical shell and hence is not strictly applicable in a theoretical study of the buckling strength of this model.

It may be of interest to consider the application to Model BR-5 of the dimensionless parameters introduced by Windenburg.[1] When the theoretical calculations were made, it was rather arbitrarily decided to disregard the portion of the weld near the toe and to consider as effective only that portion between the face of the ring and a point two-thirds of the distance from the face to the toe of the weld. Thus L was considered to be the distance between the inner third-points of the welds on adjacent rings; on this model this distance was 4.92 in. Model BR-5 was characterized by the parameters $L/2R = 0.1840$ and $h/2R = 0.00232$. This value of L together with the known values of h, R, E, and σ_y leads to a "thinness factor" λ of 1.705 and a "pressure factor" ψ of 0.315 based upon the pressure of 80 psi at which the first lobe formed. This point is plotted on ψ-λ coordinates as shown by the lower of the two points on Figure 12. The point plotted above this corresponds to the maximum load-carrying capacity of the model, which was 95 psi. In addition to these two points, two curves also appear on Figure 12: The lower of the two represents von Mises' solution for an unreinforced

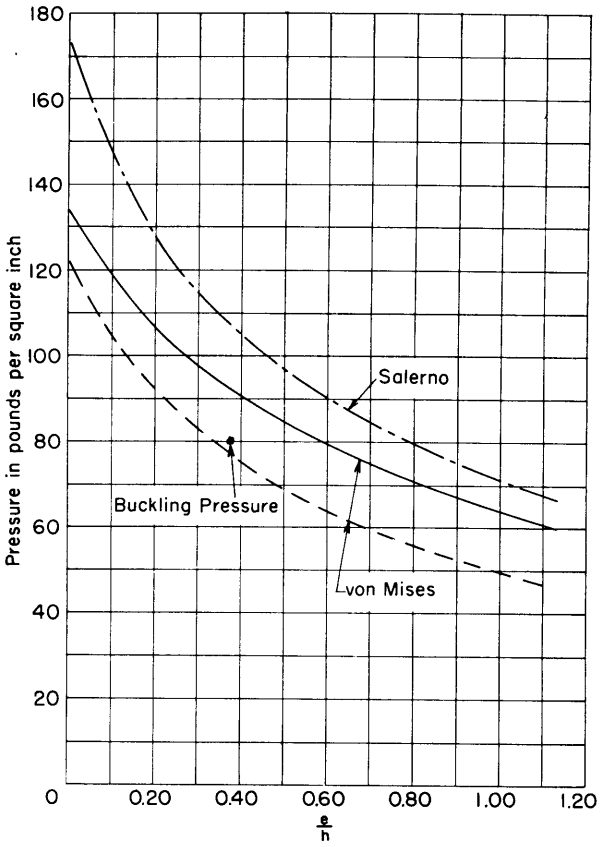

Figure 11 - Reduction in Buckling Pressure of a Geometrically Perfect Ring-Stiffened Cylindrical Shell for Various Eccentricity-Thickness Ratios (e/h) for Model BR-5, as given by Sturm's Equation

The lower curve represents the reduced pressure based upon the von Mises value of 123 psi for 16 lobes; the middle curve represents the corresponding value for a von Mises pressure of 134 psi for 14 lobes; and the upper curve represents the reduced pressure based upon Salerno's value of 173 psi for a perfect stiffened cylinder with clamped ends.

cylindrical shell, and the upper represents Salerno's solution for a cylindrical shell with clamped ends. These two curves are thought by Salerno to delineate lower and upper limits to the hydrostatic buckling pressure of an infinitely long, circular cylindrical shell reinforced by evenly spaced, perfectly rigid rings.

The tabulation of mean inward radial displacement per unit pressure at various stations in the four equal bays of Model BR-5 (presented in tabular form in Table 6) showed that the average inward radial displacement was 0.000086 in. per unit pressure midway between rings and 0.000025 in. per unit pressure at the rings. In Model BR-1, the corresponding values were 0.000071 in. and 0.000027 in., respectively. The Salerno-Pulos theory for stress distribution in a ring-reinforced cylindrical shell[10] predicts a value of 0.000083 in. per unit pressure midway between rings and 0.000037 in. per unit pressure at the rings. Therefore the inward radial displacements predicted by the Salerno-Pulos theory are 0.97 and 1.48 times the experimental values, respectively.

Points corresponding to the pressure required to cause either buckling or yielding of all known models of an unclassified nature are plotted on ψ-λ coordinates in Figure 13. For those models that failed by elastic instability, the pressure plotted is that at which the first lobe formed in the shell. The curve shown represents the relationship of the buckling pressure p expressed in terms of a dimensionless pressure factor ψ to the dimensionless parameter λ as obtained by a simplification of the von Mises equation.[6]

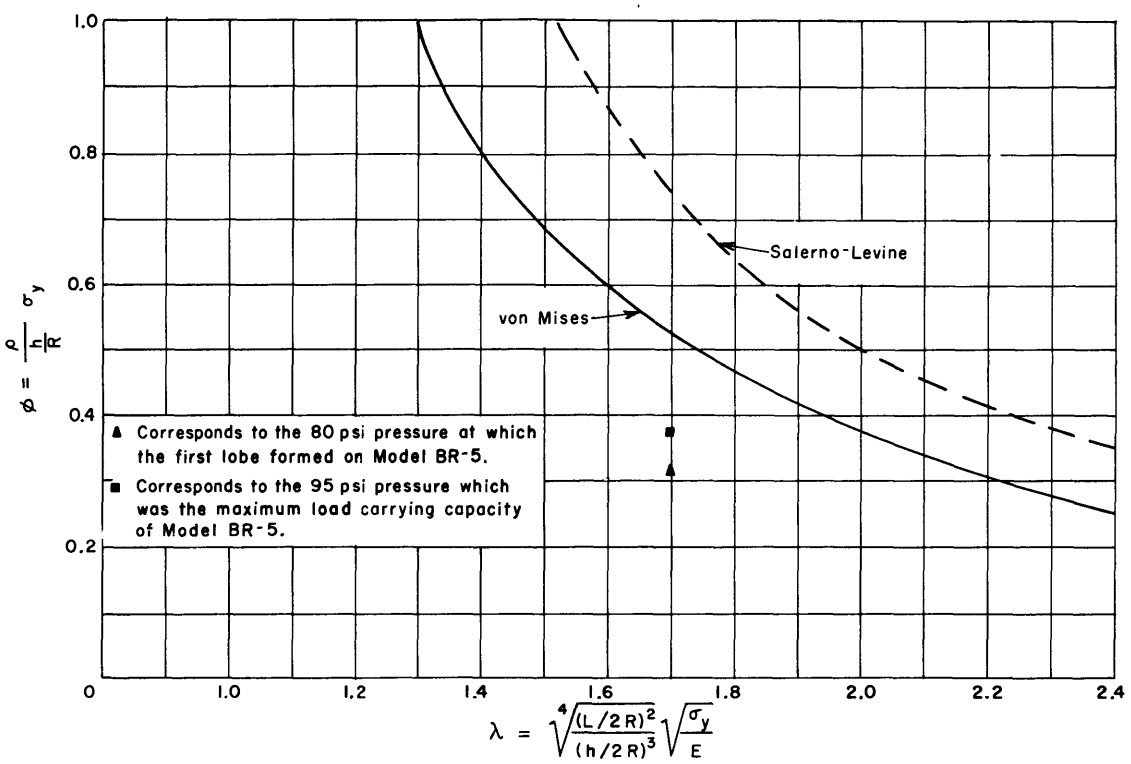

Figure 12 - Curves Representing Upper and Lower Limits of Buckling Pressure of Ring-Stiffened Cylinders Made of Steel Having a Yield Strength of 54,400 psi

COMPARISON OF MODEL BR-5 WITH MODEL BR-1 .

Models BR-5 and BR-1 were tested to destruction under the action of external hydrostatic pressure. Instability failure occurred in both models with the formation of lobes in the shell at a pressure of 80 psi. The maximum sustaining pressure was 95 psi for the BR-5 and 107 psi for BR-1. During the test of BR-5, 13 lobes formed in one of the four equal bays with space enough for one additional lobe so that 14 could have formed around the periphery of the shell if the deformations had been axisymmetric. The lobe formations in BR-1 were such that 15 or 16 could have formed around the pheriphery of the shell.

Elastic behavior was nonuniform for both models in that the radial displacements did not demonstrate a linear relationship with pressure.

Although the initial buckling pressures were the same for both models, the final mode of failure was different. Model BR-5 failed with a chain of 13 circumferential lobes between Stations 5 and 7. Model BR-1 failed after buckling by a circumferential rupture of the shell at Station 7, immediately under the toe of the weld joining the reinforcing-ring to the shell. Both failures occured in the same bay, namely Stations 5-7.

The markedly greater out-of-roundness of Model BR-1 as compared with that of BR-5 does not seem to have produced a corresponding decrease in the buckling pressure. The eccentricity-thickness ratio was 1.023 for BR-1 as compared with 0.374 for BR-5.

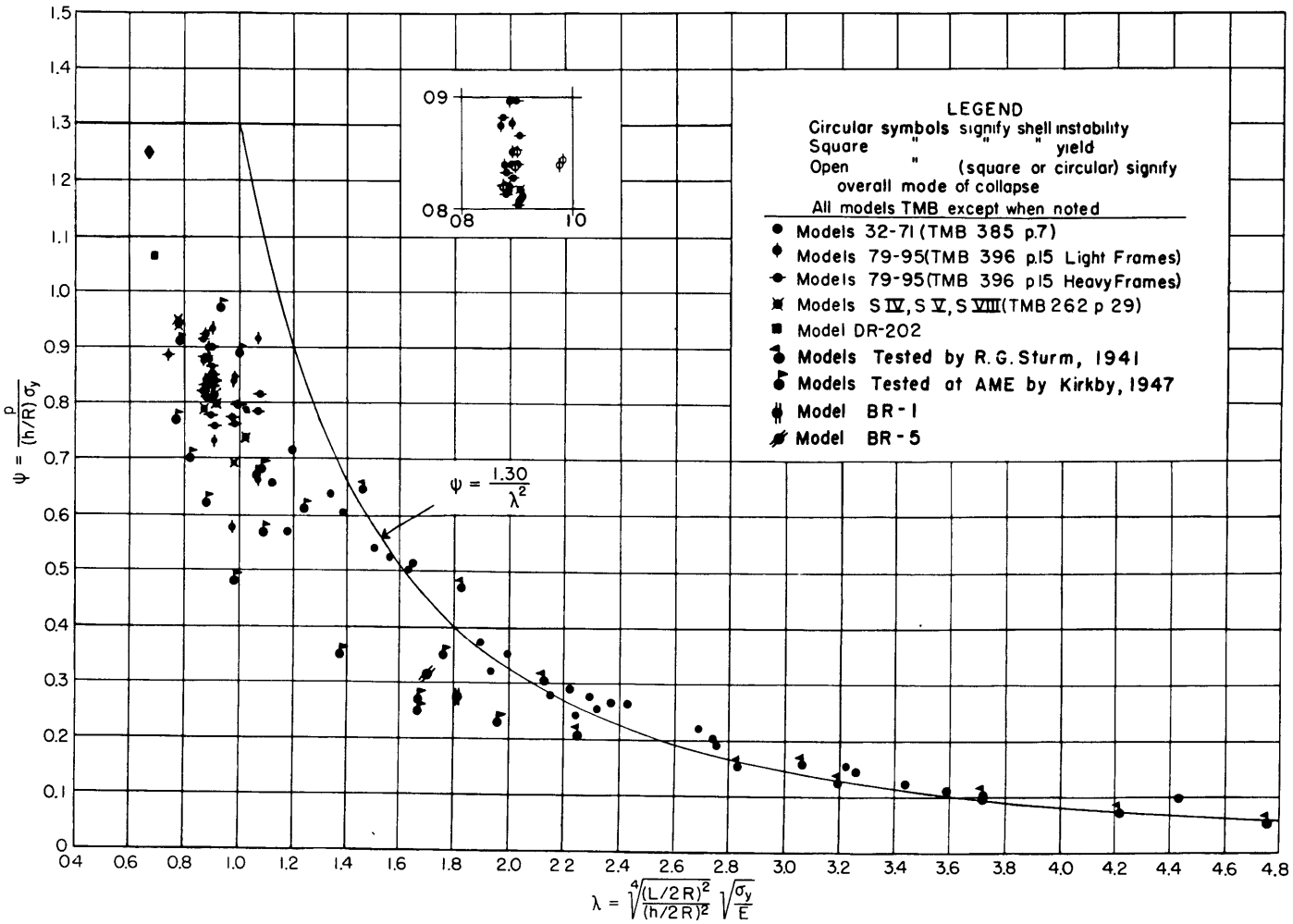

Figure 13 - Dimensionless Coordinates Used for Plotting Pressures Required to Cause Either Buckling or Yielding of Ring-Stiffened Cylindrical Shells

CONCLUSIONS

From a study of test results, the following conclusions may be drawn:

1. The elastic behavior was nonlinear at all pressures, even those below that at which buckling occurred. Measurements from the circularity contour charts showed that the radial displacements did not exhibit a linear relationship with pressure. The deformation pattern prior to buckling was mainly an exaggeration of the initial distortion of the shell such that those regions which were originally distorted inward displaced inwardly, and those initially distorted outward remained in the same position with very little displacement either inward or outward. This was true in each of the four equal bays for Models BR-5 and BR-1.

2. From an examination of the lobe formation during the test and also from the pictures, it was noted that the lobes in adjacent bays were staggered. Furthermore, with such stagger there was virtually no rotation of the generator at the two frames which contained a lobe. This mode of deformation differs considerably from the von Mises assumption of no rotational restraint at the edge of a finite cylinder but is in agreement with one of the analyses of Salerno and Levine. After pressure was relaxed following the first occurrence of buckling, the lobes did not completely disappear, so that the stability action in Model BR-5 cannot be regarded as purely elastic. The longitudinal profile of a lobe measured normal to a generator was found to be approximately of the form

$$w = C\left(1 - \cos\frac{\pi x}{\frac{L}{2}}\right)$$

where L = 4.92. An equation similar to this was found to define the longitudinal profile of a lobe measured normal to a generator during the test of BR-1.

3. The pressure at which buckling occurred (80 psi) was considerably less than that predicted by the theories of von Mises (123 psi) or Salerno and Levine (173 psi). The discrepancy in some part may be attributed to the initial out-of-roundness of the model and residual welding stresses.

4. When buckling occurred at 80 psi, lobes had formed at the regions of maximum out-of-roundness.

ACKNOWLEDGMENTS

The planning of the basic research investigation of elastic instability of ring-reinforced cylinders was under the guidance of Dr. E. Wenk, Jr. The authors would also like to express their thanks to Mr. R.L. Waterman for his assistance during conduct of the test.

The design and development of the automatic recording deflectometer used during this test and to be used during future model tests was done primarily by Dr. E. Wenk, Jr., Messrs. E.E. Johnson, W.S. Campbell, R.G. Tuckerman, J.C. Boyle, H.E. Prucha, and L.A. Lofgren.

APPENDIX 1

THE AUTOMATIC RECORDING DEFLECTOMETER

The automatic recording deflectometer is an instrument which was specially designed and built to record the circularity of cylindrical shell models at no load and also while pressure was acting on the model. A schematic diagram of the deflectometer is shown in Figure 14. The assembly and basic components are shown in Figures 15 through 19, inclusive. The basic components are

a. The tripod, which rests in a fixed position on the head of the pressure tank, (Figure 16),

b. A shaft which turns in a bushing at the center of the tripod and rests in a tapered bearing at the lower end of the shaft, (Figure 17),

c. A detachable probe (Figure 18), and

d. The recorder turntable, which includes the pen and chart-driving mechanism (Figure 19).

The shaft is driven by a 230-v, d-c reduction-gear motor; the output shaft turns at 68 rpm at rated load. The motor is shock-mounted to the tripod and powers the shaft through a worm and wheel gear. With 200 ohms resistance in the armature circuit, the shaft turns at 0.5 rpm. The probe carrier is keyed to the shaft and consequently turns with it. It can also be moved vertically along the shaft to allow positioning of the probe at various elevations during the test. In order to obtain the vertical elevations, a graduated metal tape is attached to to the probe carrier. One end of the tape is secured to the carrier, and the remaining portion of the tape is run over a small wheel, whose axis is stationary with respect to the shaft. Vertical probe positions may then be read from the metal tape. The free or loose end of the tape hangs inside the tank and is weighted so as to remain taut. The counterbalance weight also tends to relieve the downward pull due to the weight of the probe mechanism. The vertical movement of the shaft and probe is controlled by a chain drive which is operated manually; after the probe carrier has been positioned, it is held in place by braking the probe carrier against vertical movements. The top driving sprocket is attached to the upper portion of the shaft by a collar and the guiding sprocket is attached to the ring which carries the ball joint at the bottom of the shaft. The ends of the chain are attached to the probe carrier. The driving sprocket is actuated by a hand crank connected to a worm drive.

The chart on which circularity is recorded is carried on a turntable with gear teeth along its outer edge. The rotation of this chart is locked electrically to the rotation of the shaft. Two selsyn motors are used: (a) the primary, which is shock-mounted on a bracket that is welded to the tripod and (b) the secondary, which is geared to the turntable. For one turn of the selsyn on the tripod there is a corresponding turn of the selsyn on the recording turntable, which, in turn, rotates the chart. Since the gear ratio of the primary selsyn to the gear ratio of the primary selsyn to the gear on the shaft is the same as that of the secondary

selsyn to the turntable (both being 38:1), a certain angular rotation of the deflectometer shaft produces a corresponding rotation of the turntable. As long as the two selsyns are energized, the turntable is locked electrically to the shaft. If, however, they are de-energized during a test, the turntable must be repositioned. The repositioning is brought about by the secondary selsyn which locks at approximately every 9.5 deg rotation of the turntable. Repositioning is easily accomplished by placing the probe on a reference point, de-energizing the selsyn, and then placing the recording pen at the desired reference on the chart. The chart is again locked correctly to the shaft by re-energizing the selsyn.

The recording mechanism can be adjusted to indicate magnifications of 5, 10, 25, or 50 times the initial out-of-roundness of the cylindrical shell being tested. For example, if a magnification factor of 50 is used during a test and a 1.0-in. radial displacement is recorded on the circularity chart, then the radial displacement in the model at the corresponding point was 0.02 in.

The probe consists mainly of a steel case which is bolted to the probe carrier on the shaft. A small metal wheel at the end of the probe shaft is spring-loaded so that it can travel along the inner surface of the cylindrical shell, thus giving the circumferential contour of the model at a given station under a known test pressure. The probe shaft acts as the core of a differentially wound transformer which has been installed inside the metal casing. The secondary output of the differential transformer is fed into an electronic bridge circuit which energizes a pen motor drive; this, in turn, positions the pen on the circularity chart. By virtue of the radial positioning of the pen plus the angular rotation of the turntable, a circularity curve is traced.

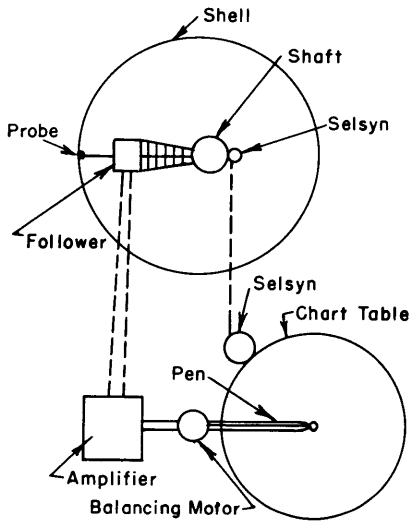

Figure 14 - Schematic Diagram of Automatic Recording Deflectometer

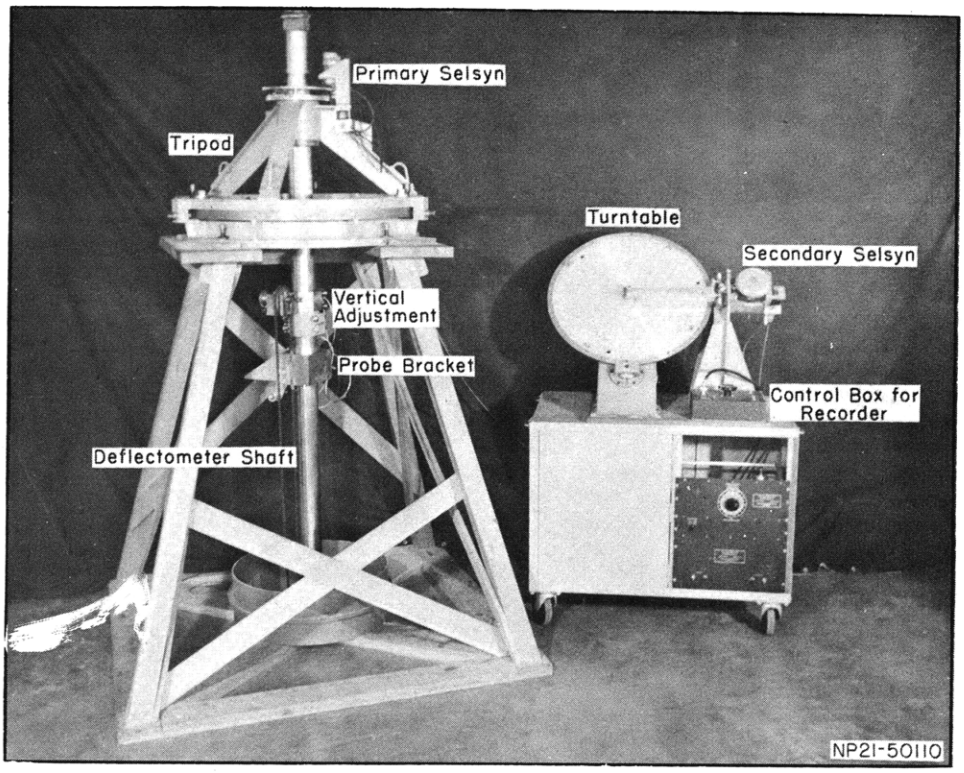

Figure 15 - Assembly of Automatic Recording Deflectometer

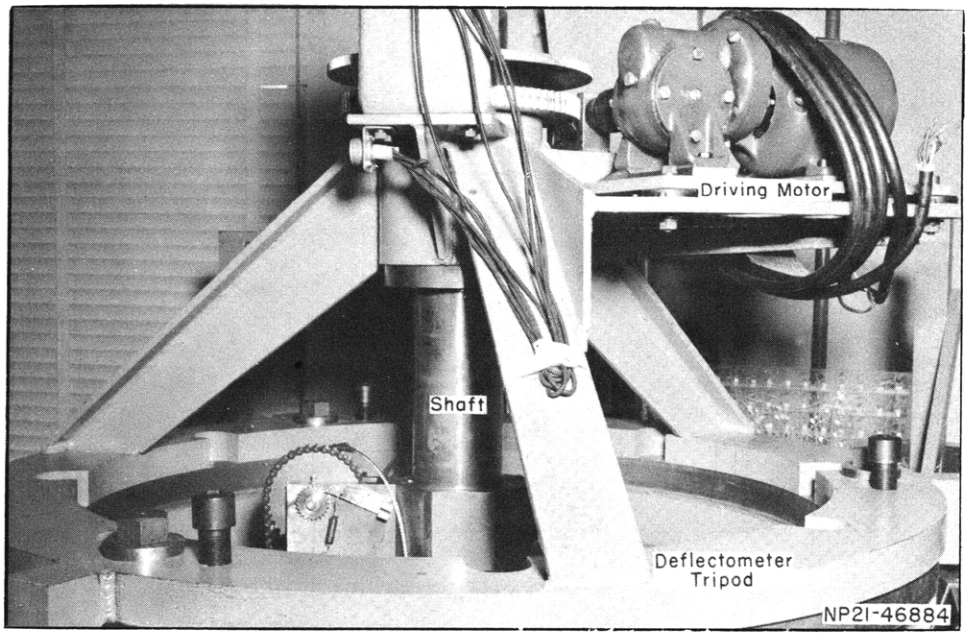

Figure 16 - Tripod, Shaft, and Driving Motor of Automatic Recording Deflectometer

The tripod rests upon the top of the 37-in.-diameter hydrostatic-pressure test tank.

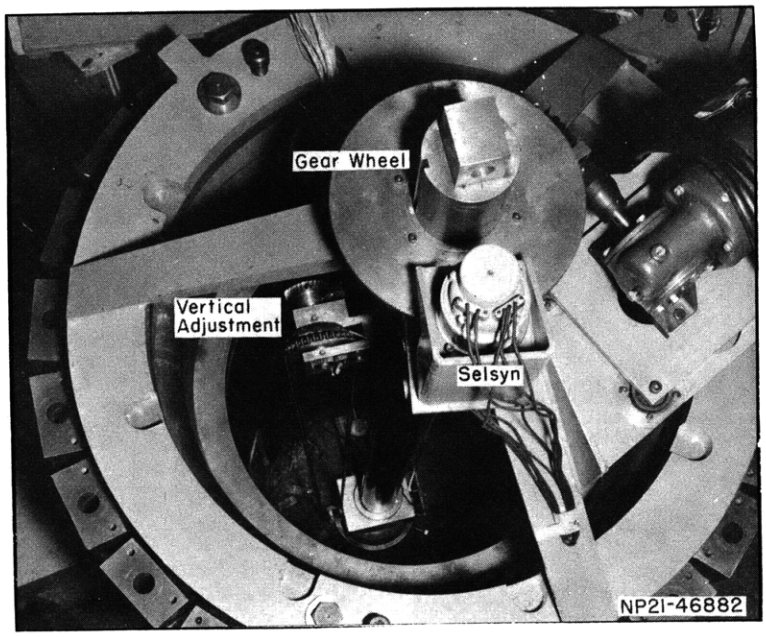

Figure 17 - Top View of Automatic Recording Deflectometer Looking Down into Test Tank

This view shows how the tripod rests upon the top of the test tank and also how the vertical shaft is centered within the model.

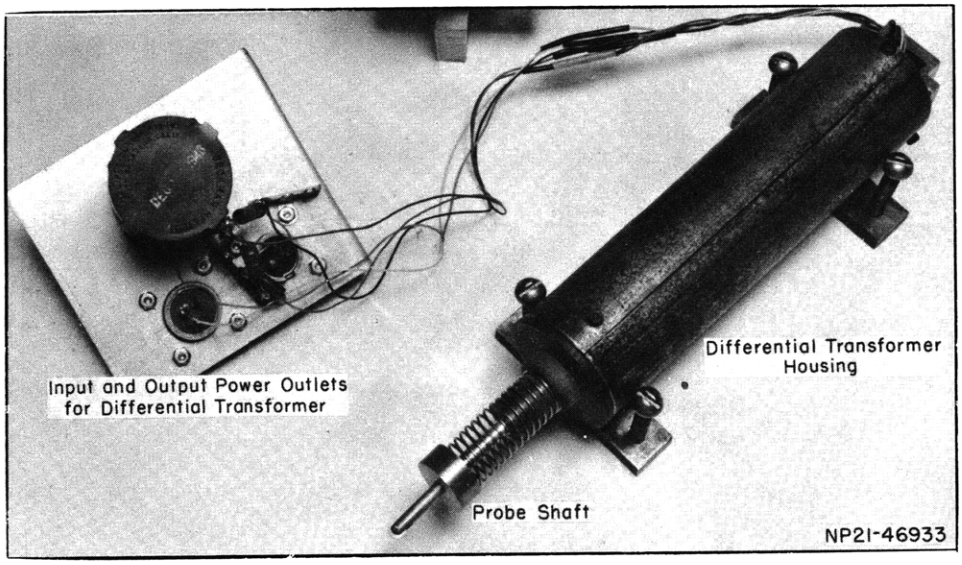

Figure 18 - Probe of Automatic Recording Deflectometer

The probe is maintained in an outward position by means of the spring. The small metal wheel at the end of the probe shaft is in contact with the interior of the cylindrical shell while traversing the periphery of the shell.

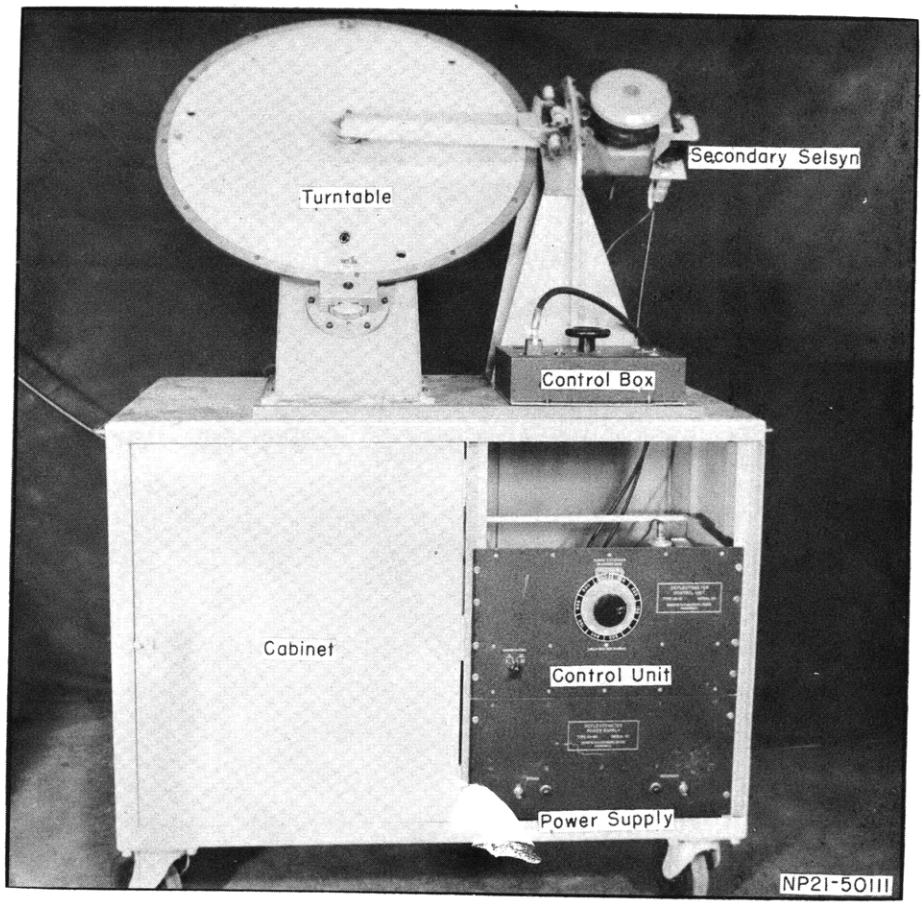

Figure 19 - Recorder Turntable, Pen, and Chart-Driving Mechanism of the Automatic Recording Deflectometer

A chart is placed on the turntable and, as the probe traverses the inner surface of the shell, a contour is traced on the chart at a predetermined magnification.

APPENDIX 2

CIRCULARITY CONTOURS AT EACH STATION ON MODEL BR-5

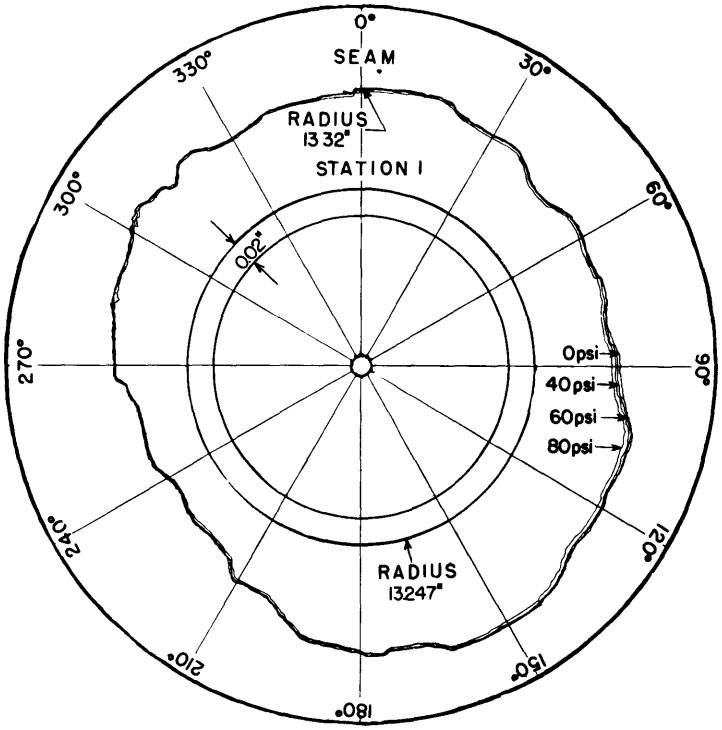

Figure 20 - Circularity Contours at Station 1

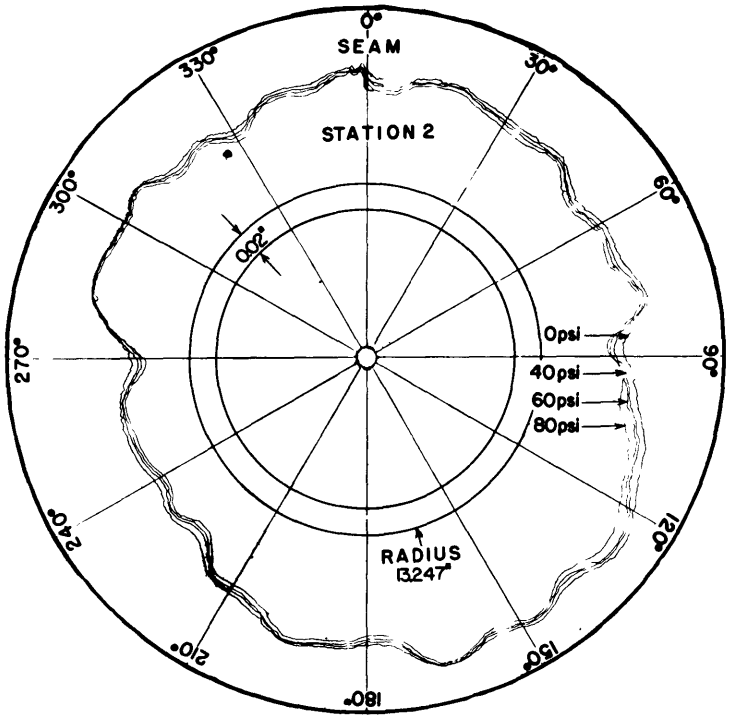

Figure 21 - Circularity Contours at Station 2

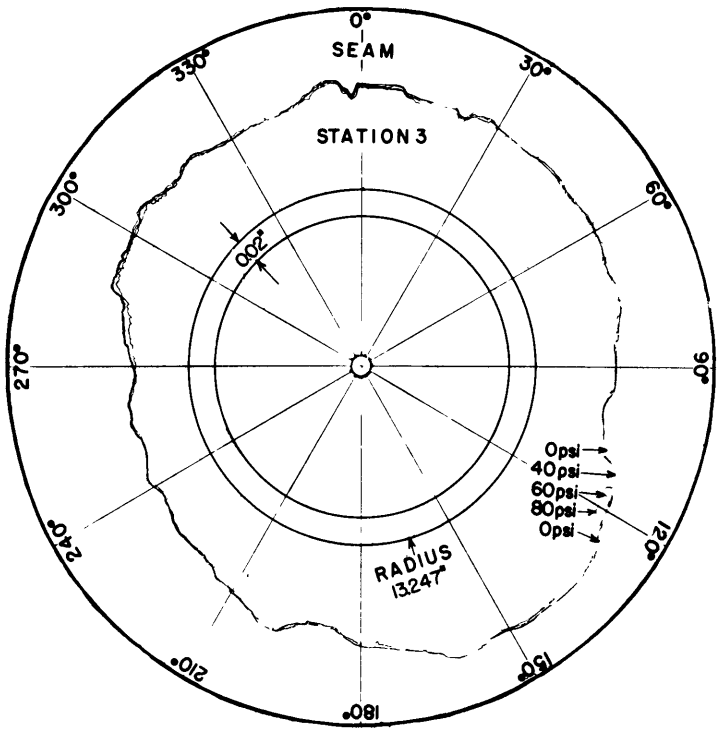

Figure 22 - Circularity Contours at Station 3

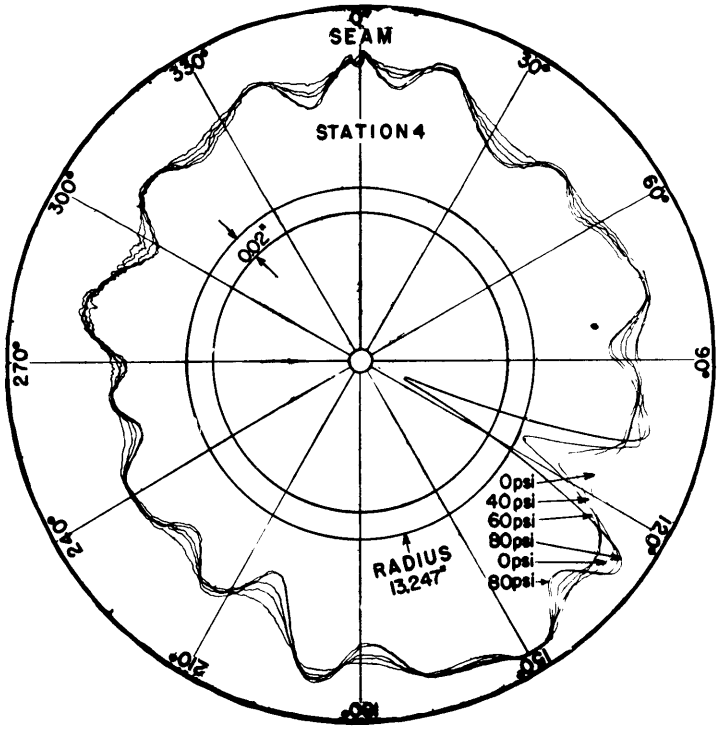

Figure 23 - Circularity Contours at Station 4

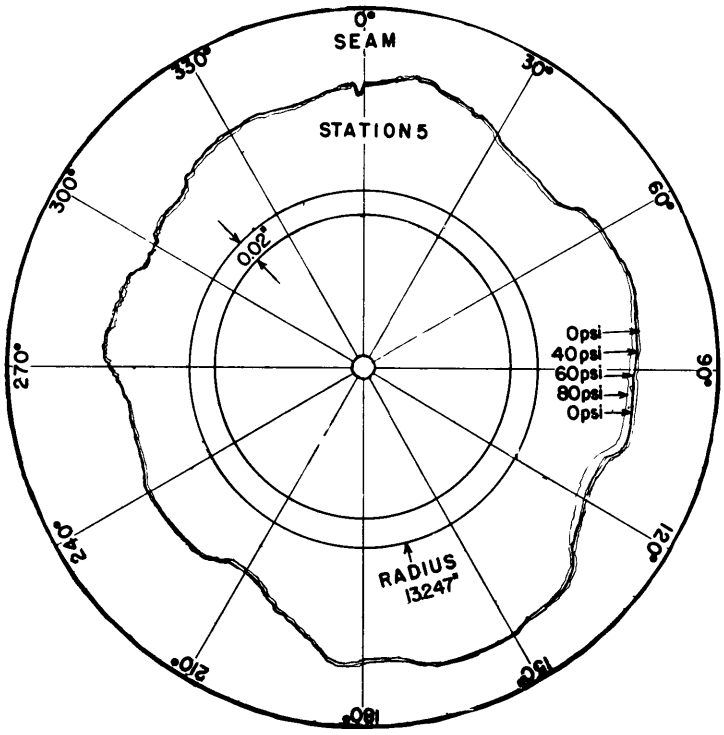

Figure 24 - Circularity Contours at Station 5

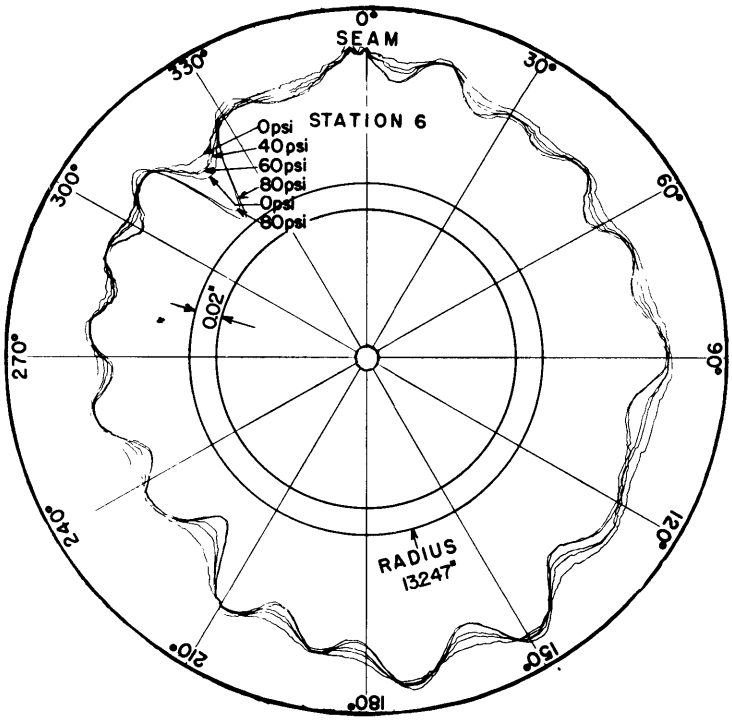

Figure 25 - Circularity Contours at Station 6

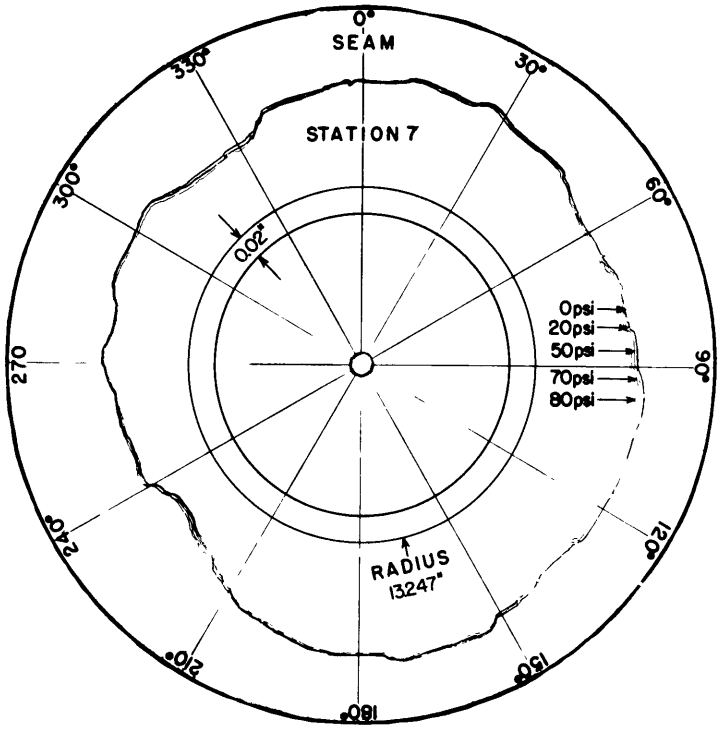

Figure 26 - Circularity Contours at Station 7

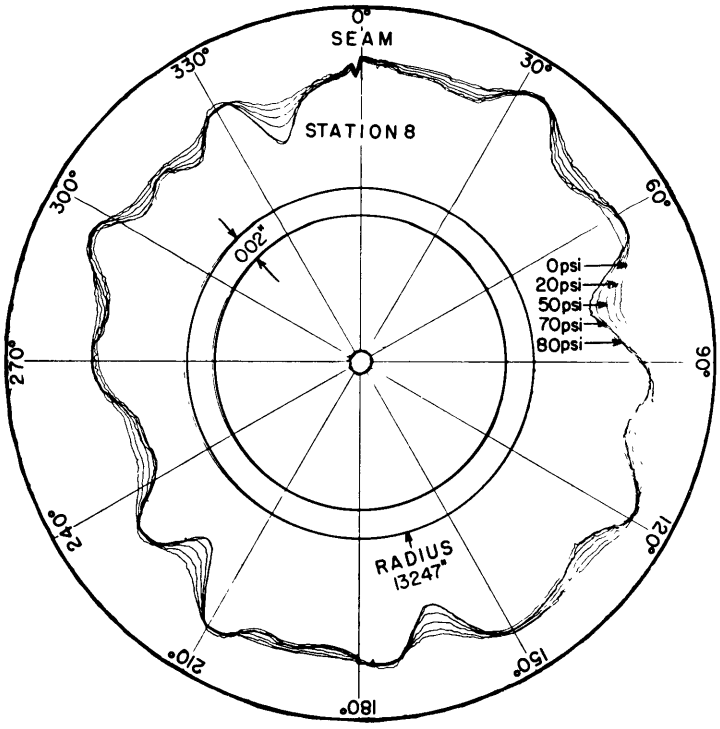

Figure 27 - Circularity Contours at Station 8

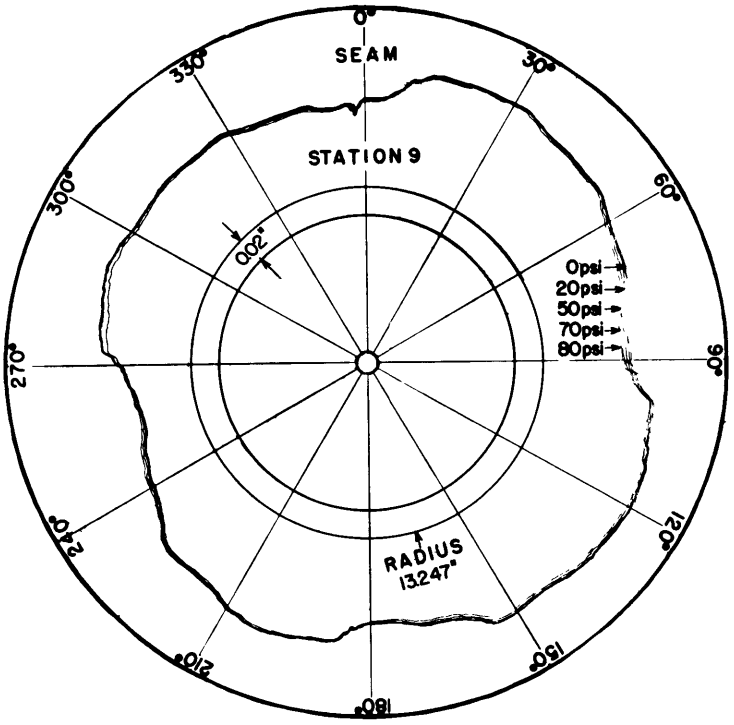

Figure 28 - Circularity Contours at Station 9

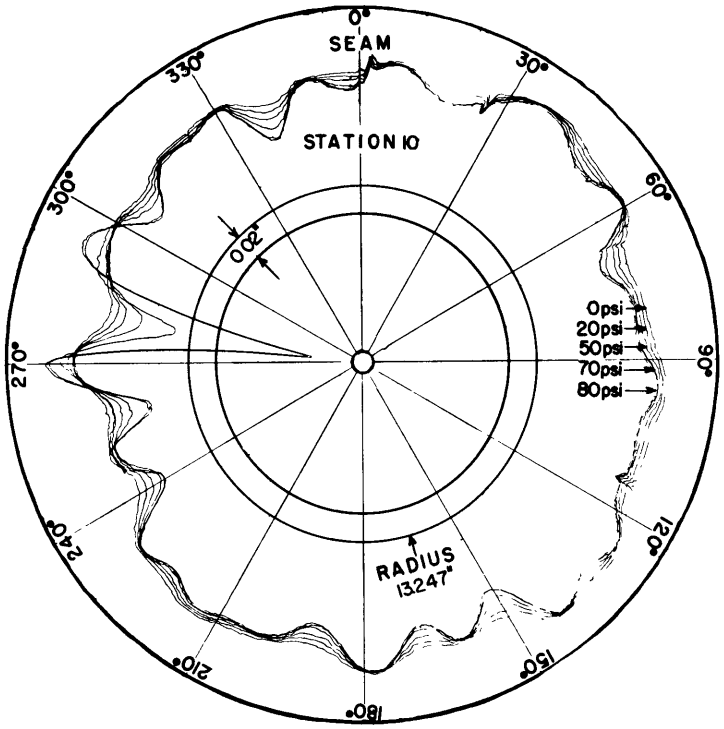

Figure 29 - Circularity Contours at Station 10

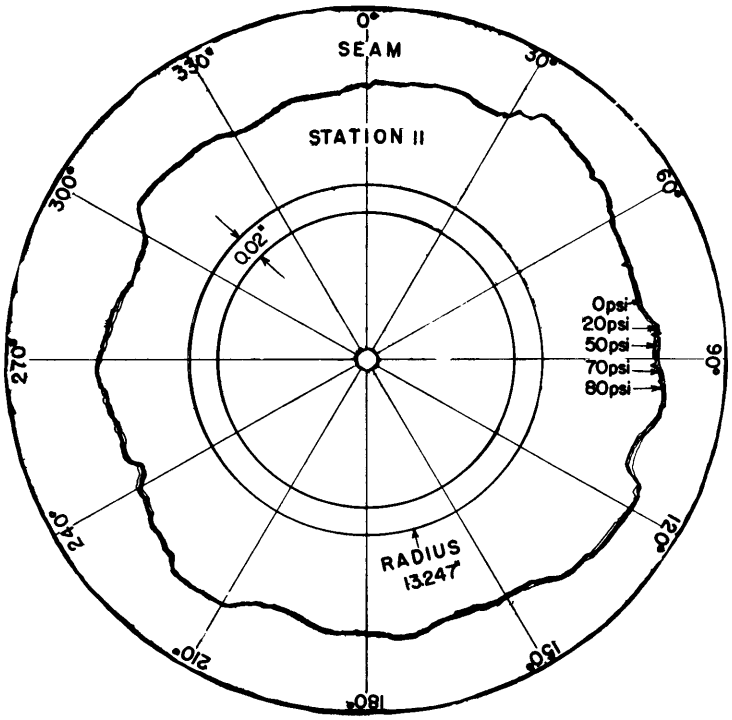

Figure 30 - Circularity Contours at Station 11

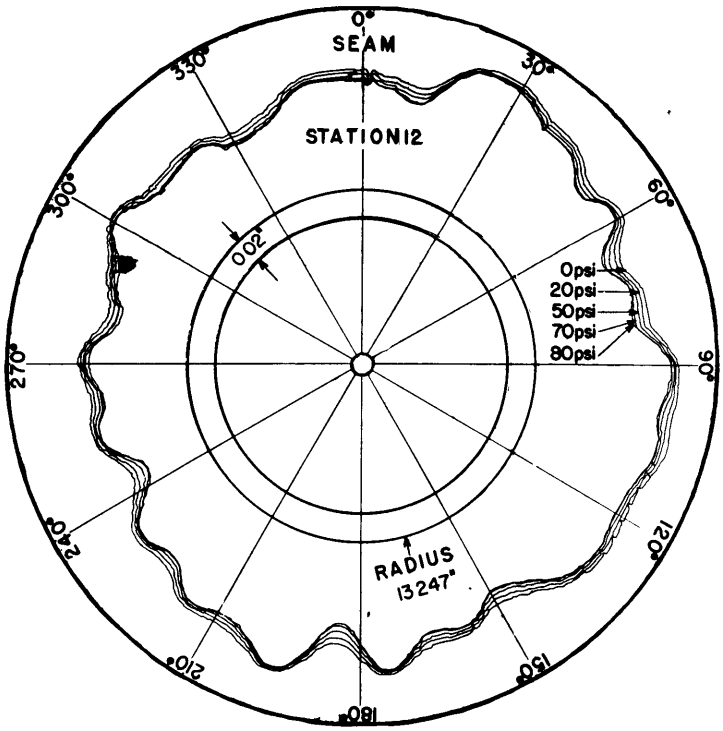

Figure 31 - Circularity Contours at Station 12

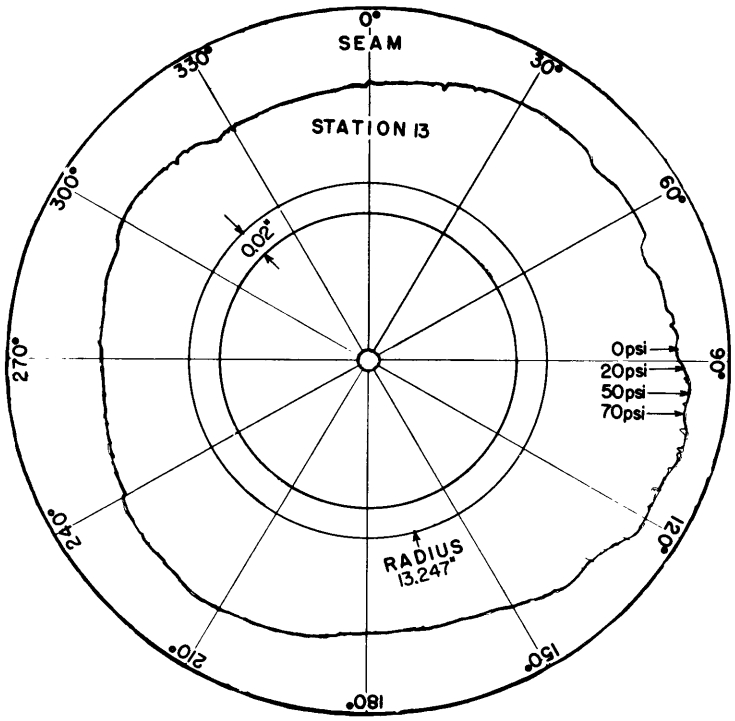

Figure 32 - Circularity Contours at Station 13

REFERENCES

1. Windenburg, D.F., and Trilling, C., "Collapse by Instability of Thin Cylindrical Shells Under External Pressure," Trans. A.S.M.E., Vol. 56, No. 11, 1934 (TMB Report 385, July 1934).

2. Nash, W.A., and Wenk, E., Jr., "Tests of the Elastic Stability of a Ring-Stiffened Cylindrical Shell, Model BR-1 (λ = 1.82), Subjected to Hydrostatic Pressure," TMB RESTRICTED Report C-439, March 1953.

3. National Bureau of Standards "Report on Compressive Tests of Fourteen Steel Specimens Submitted by the David Taylor Model Basin," NBS Lab. No. 6.416-237, 3 July 1950.

4. TMB Plan E-498-1 "Cylindrical Shell, Ring Reinforced, Model No. BR-1," 22 January 1951.

5. Holt, M., "A Procedure for Determining the Allowable Out-of-Roundness for Vessels Under External Pressure," Trans. A.S.M.E., Vol. 74, No. 7, October 1952.

6. von Mises, R., "Det kritische Aussendruck für allseits belastete zylindrische Rohre," Fest. zum 70 Geburtstag, von Prof. Dr. A. Stodola, Zurich, 1929, pp. 418-430.

7. Tokugawa, T., "Model Experiments on the Elastic Stability of Closed and Cross-Stiffened Circular Cylindres Under Uniform External Pressure," Proc. World Engrg. Congress, Tokyo, 1929, Vol. 29, pp. 249-279.

8. Salerno, V.L., and Levine, B., "The Determination of the Hydrostatic Buckling Pressures for Circular Cylindrical Shells Reinforced with Rings," PIBAL Report 182, 1951.

9. Sturm, R.G., "A Study of the Collapsing Pressure of Thin-Walled Cylinders," University of Illinois Engineering Experiment Station Bulletin No. 329, 1941.

10. Salerno, V.L., and Pulos, J.G., "Stress Distribution in a Circular Cylindrical Shell Under Hydrostatic Pressure Supported by Equally Spaced Circular Ring Frames," PIBAL Report No. 171-A, 1951.

INITIAL DISTRIBUTION

Copies	
14	Chief, Bureau of Ships, Technical Library (Code 327), for distribution: 5 Technical Library 1 Technical Assistant to Chief of Bureau (Code 106) 1 Preliminary Design and Ship Protection (Code 420) 1 Preliminary Design (Code 421) 1 Underwater Explosion Research (Code 423) 1 Hull Design (Code 440) 2 Scientific, Structural and Hydromechanics (Code 442) 2 Submarines (Code 515)
2	Chief of Naval Research, Mechanics and Materials Branch
2	Commander, U.S. Naval Ordnance Laboratory, White Oak, Silver Spring 19, Md.
1	Director, U.S. Naval Research Laboratory, Anacostia, Washington 25, D.C.
2	Commander, Norfolk Naval Shipyard, Underwater Explosions Research Division, (Code 290), Portsmouth, Va.
2	Commander, Portsmouth Naval Shipyard, Portsmouth, N.H.
2	Commander, U.S. Naval Ordnance Test Station, Inyokern, China Lake, Calif.
1	Commanding Officer, U.S. Naval Underwater Ordnance Station, Newport, R.I.
2	Commander, Mare Island Naval Shipyard, Vallejo, Calif.
3	Supervisor of Shipbuilding, USN, and Naval Inspector of Ordnance, Groton, Conn.
1	Director, U.S. Naval Engineering Experiment Station, Annapolis, Md.
1	Chief, Armed Forces Special Weapons Project, Dept. of Defense, P.O. Box 2610, Washington, D.C.
1	Director, Langley Aeronautical Laboratory, Langley Air Force Base, Va.
1	Commanding General, Headquarters, Air Materiel Command, Wright-Patterson Air Force Base, Ohio
2	Chairman, Research and Development Board, Dept. of Defense Bldg., Washington 25, D.C.
1	Prof. Jesse Ormondroyd, Dept. of Engineering Mechanics, University of Michigan, Ann Arbor, Mich.
1	Dr. N.J. Hoff, Department of Aeronautical Engineering and Applied Mechanics, Polytechnic Institute of Brooklyn, 99 Livingston St., Brooklyn 2, N.Y.
1	Dr. J.N. Goodier, School of Engineering, Stanford University, Stanford, Calif.
1	Dr. F.K. Teichmann, Department of Aeronautical Engineering, New York University, New York, N.Y.
1	Dr. C.T. Wang, Department of Aeronautical Engineering, New York University, New York, N.Y.
1	Dr. E. Sternberg, Illinois Institute of Technology, Technology Center, Chicago 16, Ill.
1	Dr. W. Prager, Graduate Division of Applied Mathematics, Brown Univeristy, Providence, R.I.

1	Dr. W.H. Hoppmann, Department of Applied Mechanics, Johns Hopkins University, Baltimore, Md.
1	Prof. R.M. Hermes, University of Santa Clara, Santa Clara, Calif.
1	Dr. R.P. Petersen, Director, Applied Physics Division, Sandia Laboratory, Albuquerque, New Mexico
1	Dr. F.H. Clauser, Department of Aeronautics, The Johns Hopkins University, Baltimore, Md.
1	Prof. Lloyd Donnell, Department of Mechanics, Illinois Institute of Technology, Technology Center, Chicago 16, Ill.
1	Dr. Bruce Johnston, 301 West Engineering Building, University of Michigan, Ann Arbor, Mich.
1	Dr. N.M. Newmark, Structural Research Division, University of Illinois, Urbana, Ill.
1	Prof. T.J. Dolan, Department of Theoretical and Applied Mechanics, University of Illinois, Urbana, Ill.
1	Dr. R.D. Mindlin, Columbia University, New York, N.Y.
1	Mr. F.V. Hartman, The Aluminum Ore Co., 3300 Missouri Ave., East St. Louis, Ill.
1	Dr. R.G. Sturm, Alabama Polytechnic Institute, Auburn Research Foundation and Engineering Experiment Station, Textile Engineering Building, Auburn, Ala.
1	Dr. Dana Young, Mechanical Engineering Department, University of Minnesota, Minneapolis 14, Minn.
1	Prof. E.O. Waters, Yale University, New Haven, Conn.
1	Dr. M. Hetényi, Northwestern University, Technological Institute, Evanston, Ill.
1	Mr. H.C. Boardman, Chicago Bridge and Iron Company, 1305 West 105th St., Chicago 43, Ill.
1	Mr. W.R. Burrows, Standard Oil Company of Indiana, Whiting, Ind.
1	Mr. M.B. Higgins, The Texas Company, 135 East 42nd Street, New York 17, N.Y.
1	Dr. Marshall Holt, Aluminum Research Laboratories, P.O. Box 772, New Kensington, Pa.
1	Mr. E.C. Korten, Hartford Steam Boiler Inspection and Insurance Company, Hartford, Conn.
1	Mr. H.L. O'Brien, Graver Tank and Manufacturing Company, 4130 Todd, East Chicago, Ind.
1	Mr. D.B. Wesstrom, Design Division, Engineering Department, E.I. duPont de Nemours and Company, Wilmington 98, Del.
1	Applied Physics Laboratory, The Johns Hopkins University, 8621 Georgia Ave., Silver Spring, Md.
1	The Babcock and Wilcox Co., Research and Development Dept., Alliance, Ohio
3	Pressure Vessel Research Committee, 29 West 39th St., New York, N.Y.
1	Dr. James R. Adams, Development Engineer, Midvale Company, Nicetown, Philadelphia 40, Pa.
1	Mr. Perry R. Cassidy, The Babcock and Wilcox Company, 80 Federal St., Boston 10, Mass.

1 Mr. Harold O. Hill, Assistant Chief Engineer, Fabricated Steel Construction, Bethlehem Steel Company, Bethlehem, Pa.

1 Mr. Henry Liessenberg, Stress Research Engineer, Combustion Engineering-Superheater, Inc., 200 Madison Ave., New York 16, N.Y.

1 Mr. Frank L. Maker, Engineering Specialist, California Research and Development Company, 200 Bush St., San Francisco, Calif.

1 Mr. James J. Murphy, Section Engineer, Development Division, M.W. Kellogg Company, 225 Broadway, New York 7, N.Y.

1 Mr. Cyril O. Rhys, Sr., Independent Consultant, 160 Mountain Ave., Westfield, N.J.

1 Mr. G.J. Schoessow, Babcock and Wilcox Company, Barberton, Ohio

1 Mr. W. Spraragen, Director, Welding Research Council, 29 West 39th St., New York 18, N.Y.

1 Mr. George W. Watts, Director of Engineering, Standard Oil Company (Indiana) 910 S. Michigan Ave., Chicago 80, Ill.

9 British Joint Services Mission (Navy Staff), P.O. Box 165, Benjamin Franklin Station, Washington, D.C.

1 British Shipbuilding Research Association, 5 Chesterfield Gardens, Curzon St., London, W.1, England

NAVY-DPPO PRNC WASH D C